



THE UNIVERSITY OF ARIZONA

Wyant College  
of Optical Sciences

SAND2019-14332PE



▶ **NOVEL HYBRID ANALYSIS TECHNIQUES FOR  
COMPLEX OPTICAL SYSTEMS**

**Brian Redman**

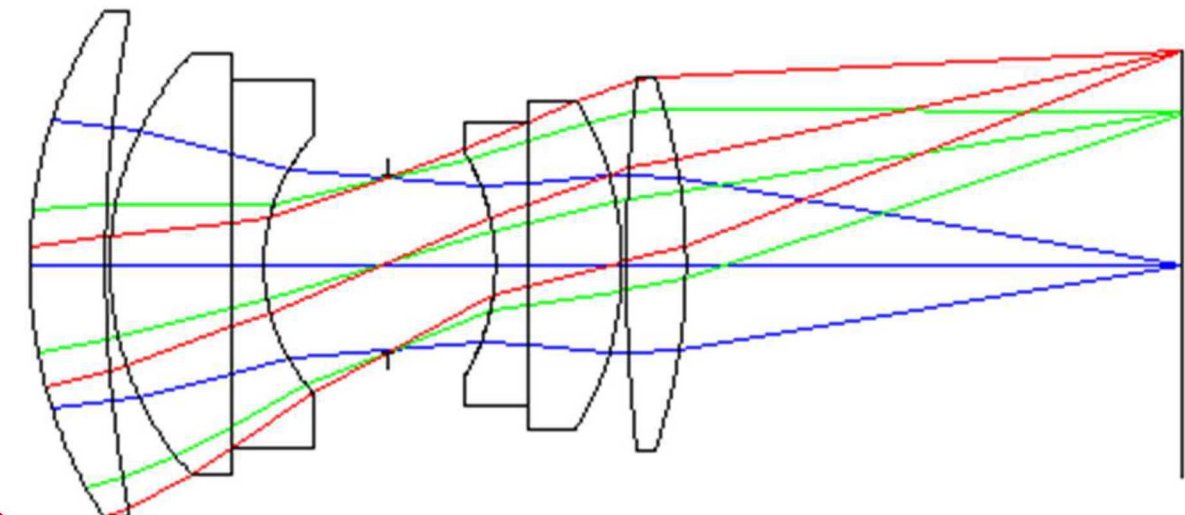
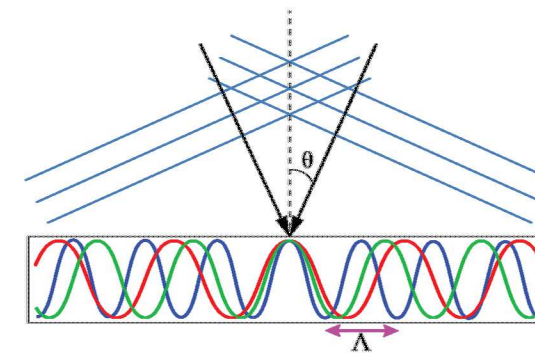
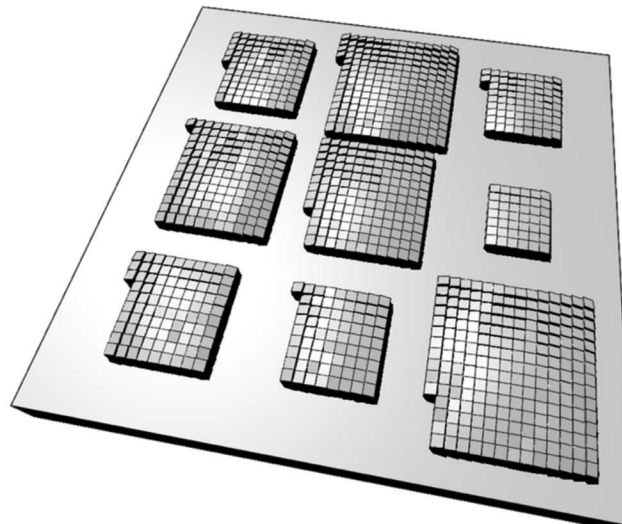


Sandia National Laboratories is a multimission laboratory managed and operated by National Technology & Engineering Solutions of Sandia, LLC, a wholly owned subsidiary of Honeywell International Inc., for the U.S. Department of Energy's National Nuclear Security Administration under contract DE-NA0003525.

# Leveraging traditional techniques to model complex optical systems

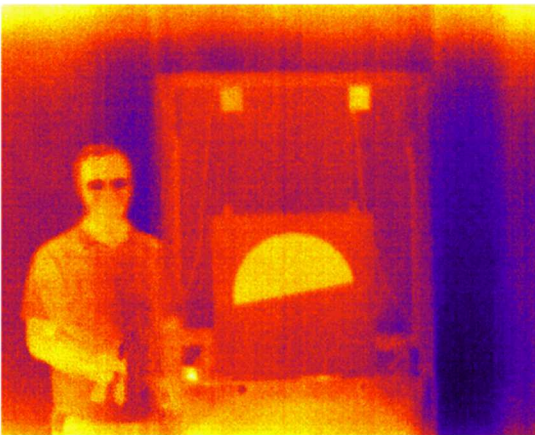


- Extensive work optimizing modeling and measurement techniques for traditional optical systems
- New methods required for non-traditional optical systems
  - Combination of traditional processing and custom analysis techniques can be used to efficiently simulate complex optical systems

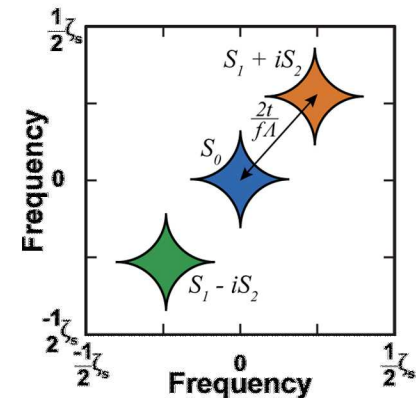
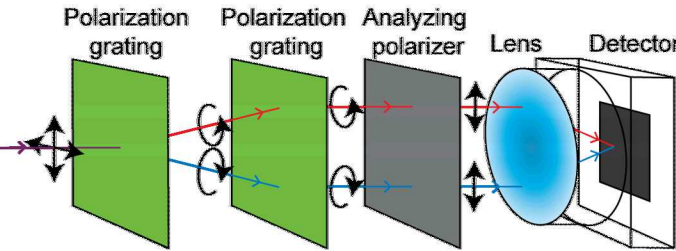


# Modeling and measurements of Four optical systems

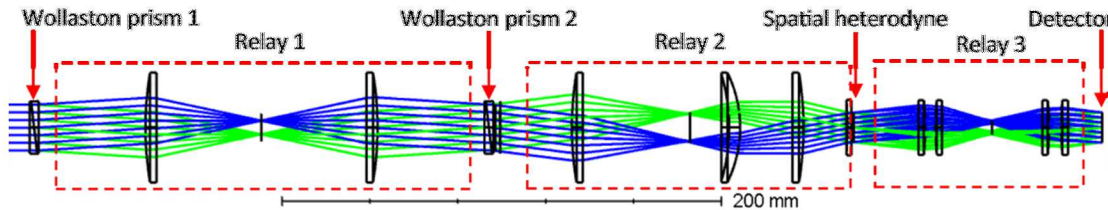
## 1. Long-wave infrared measurement of image degradation caused by fog



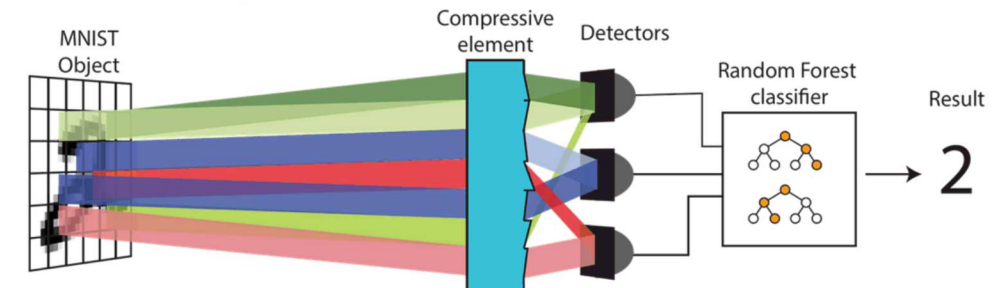
## 2. Channeled imaging polarimeter



## 3. Long-wave infrared snapshot Fourier transform spectrometer

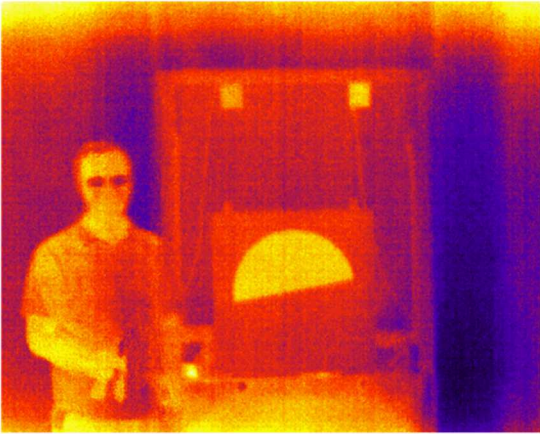


## 4. Compressive classification

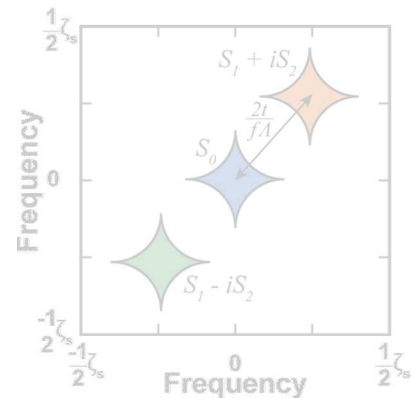
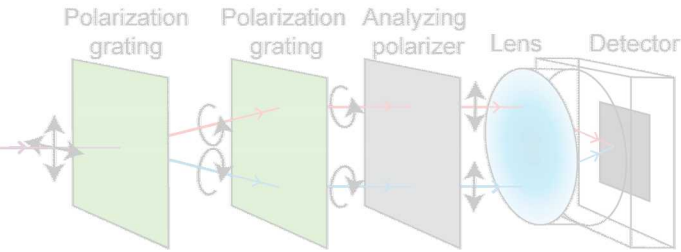




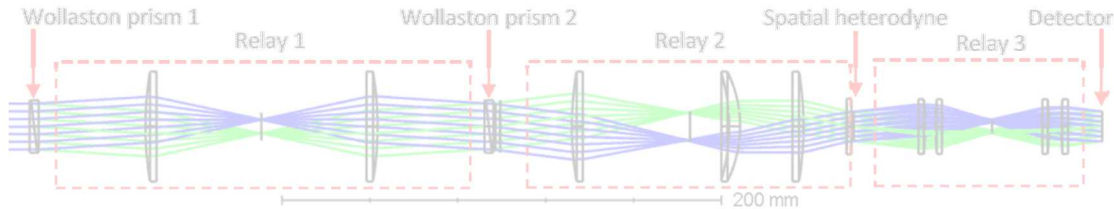
## 1. Long-wave infrared measurement of image degradation caused by fog



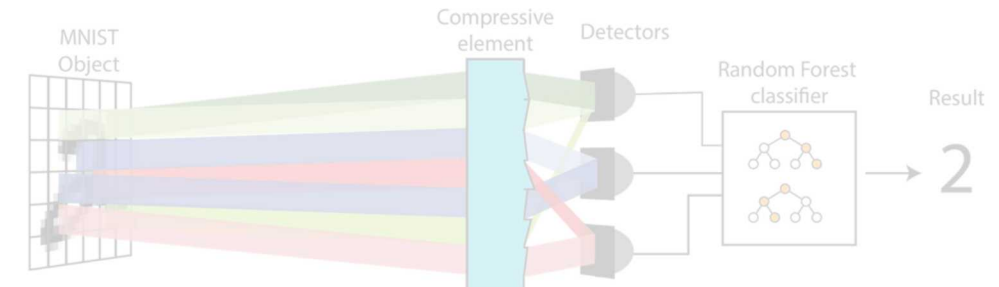
## 2. Channeled imaging polarimeter



## 3. Long-wave infrared snapshot Fourier transform spectrometer



## 4. Compressive classification

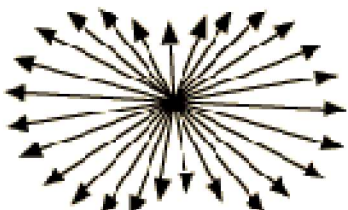


# Reduced awareness due to fog causes accidents

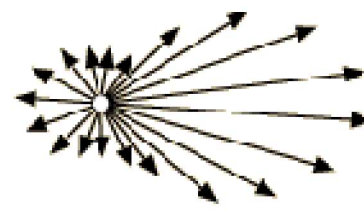


75-Car Pile-Up Kills at Least 3  
ABC News March 31, 2013

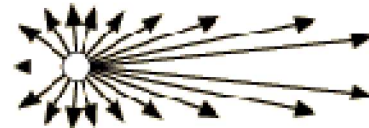
Rayleigh Scattering



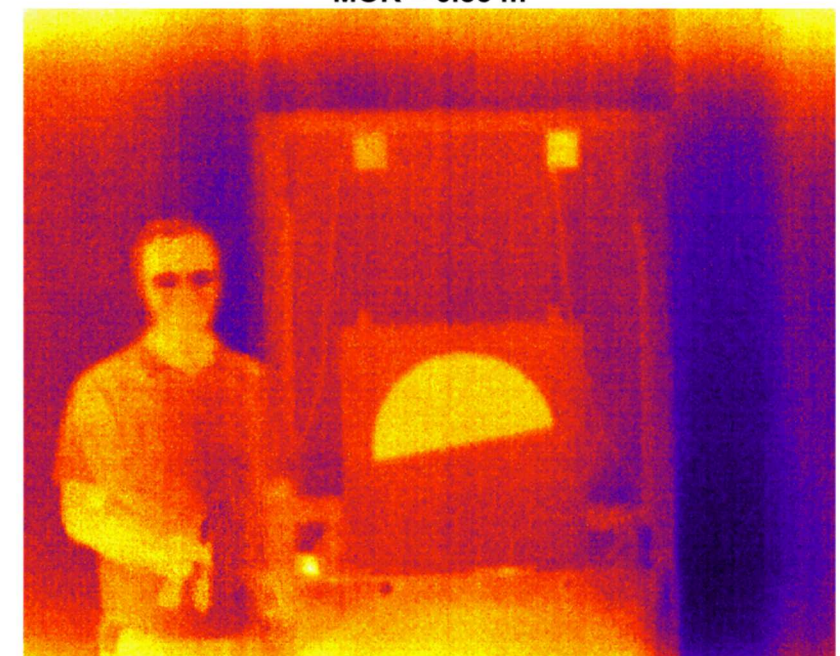
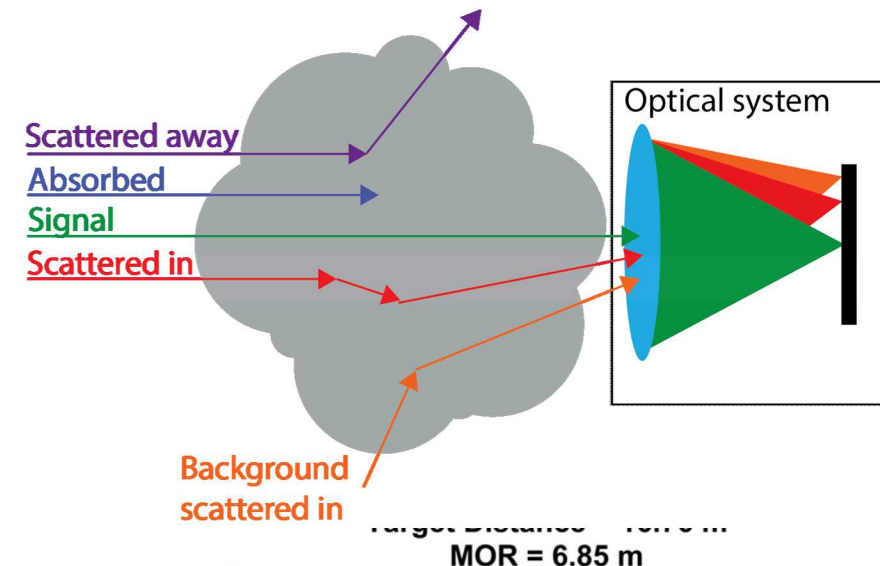
Mie Scattering



Mie Scattering,  
larger particles



→ Direction of incident light



# How imaging through fog is currently addressed

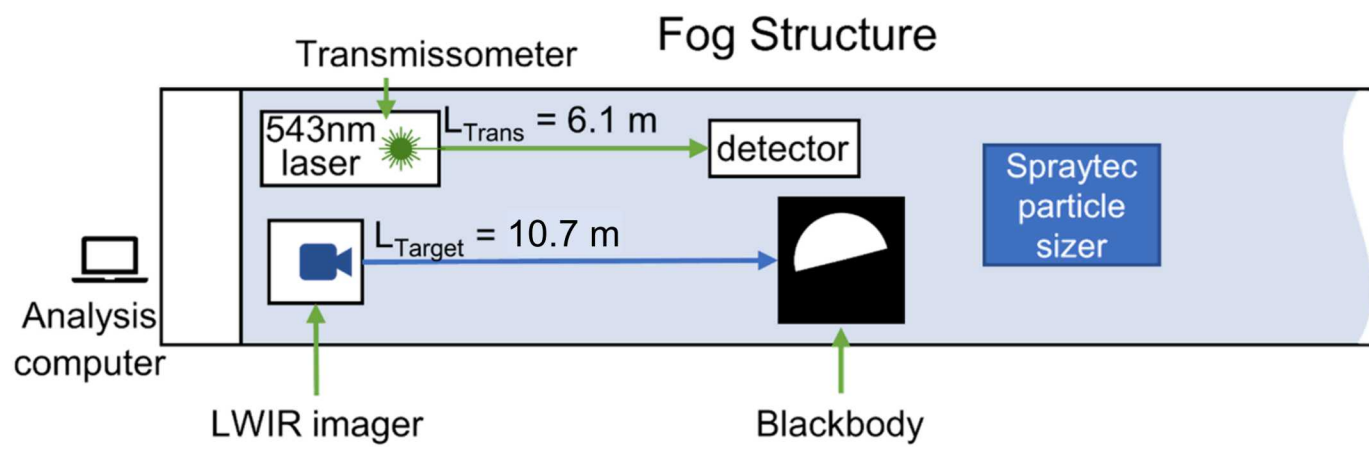
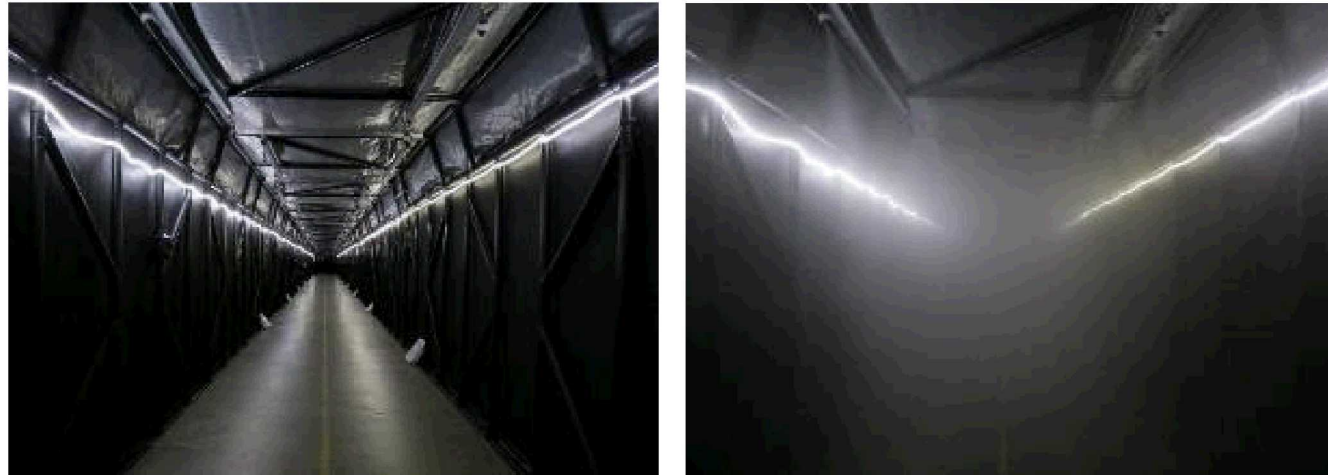
- **Visibility**
  - Distance that an object can be seen
- **Koshmieder's Law**
  - Dark object against light background
  - Daytime contrast against the sky
  - Approximated using transmission
- **Allard's Law**
  - Transmission of point source
  - Distance that a lighthouse is visible
  - Nighttime visibility of runway lights
- **Meteorological optical range**
  - 2,700 K lamp
  - Distance to attenuate a collimated beam
  - 5% transmission



# Sandia National Labs fog facility enables repeatable measurements

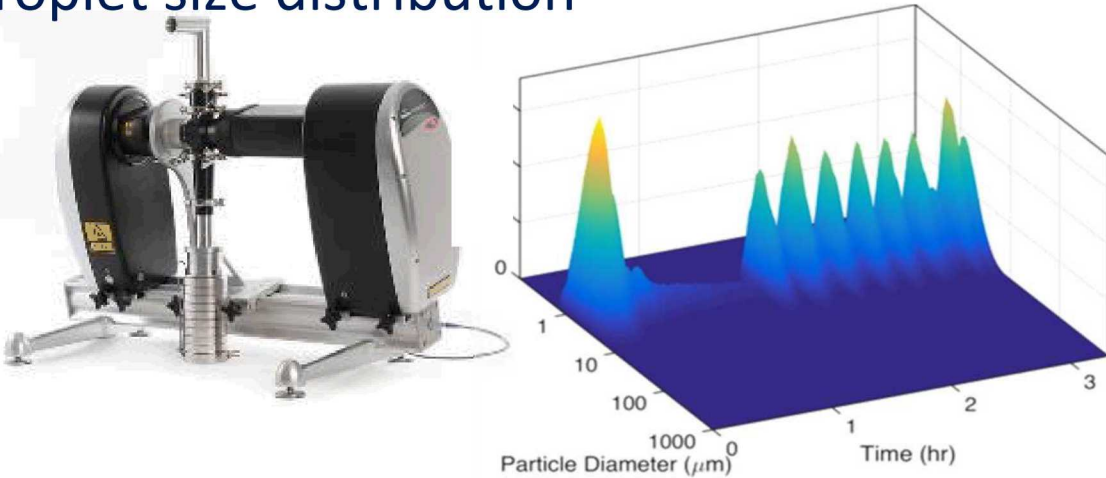


- Fog facility
  - One of the largest facilities in the world
  - 3m x 3m x 55 m
  - Extremely thick fog
  - Generation dissipation cycles
- LWIR measurements
  - Slant edge to measure MTF
  - Isolates blurring



# A combination of instruments is required to characterize the fog

Malvern Spraytec measures droplet size distribution



Transmissometer measures extinction over a long distance

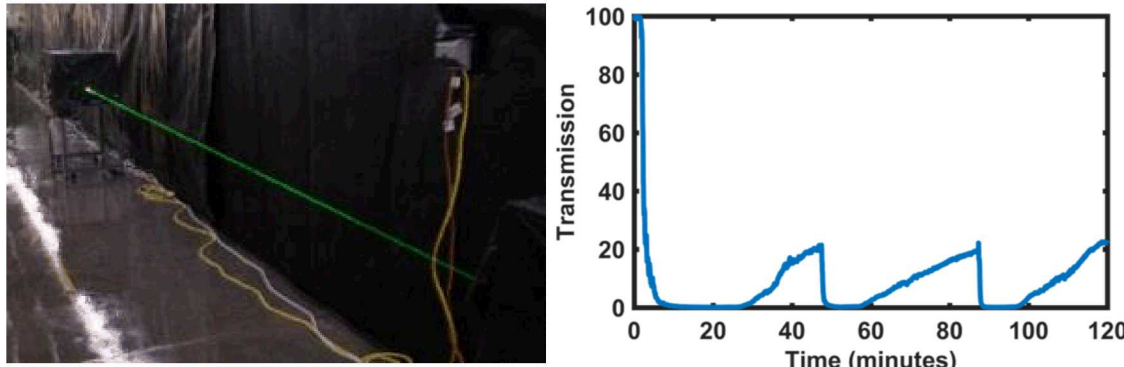
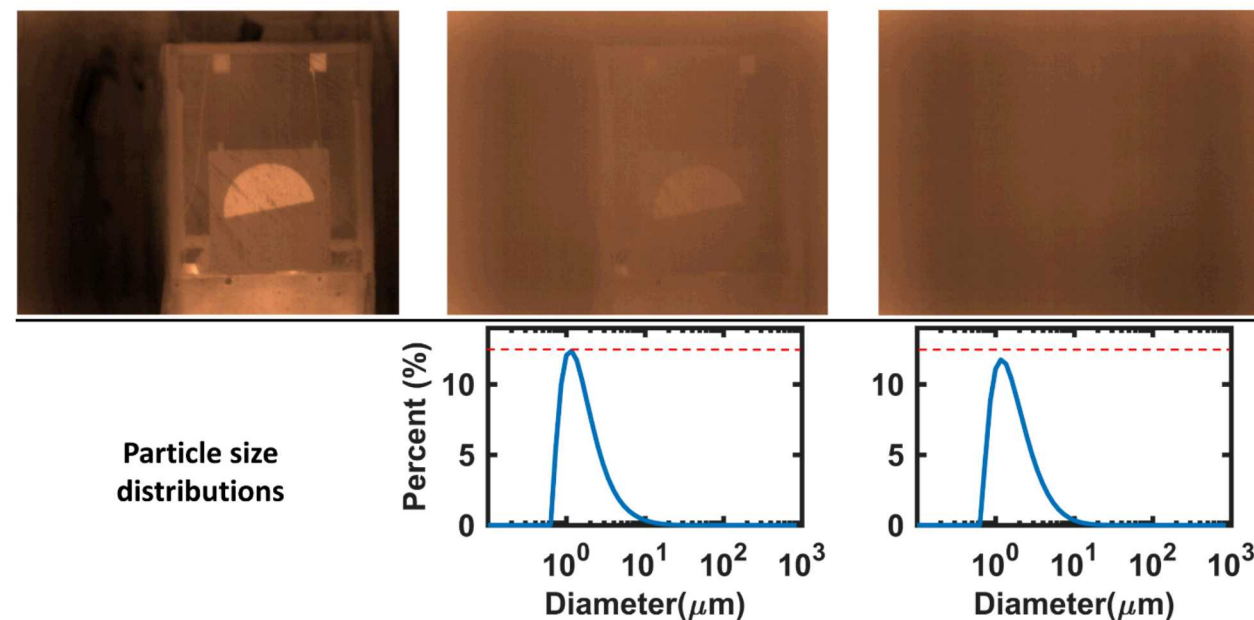


Image measurements synced to fog parameters



Parameters of the fog

$\text{MOR}_{543} = 6.00 \text{ m}$   
 $\text{LWC} = 0.53 \text{ g/m}^3$   
 $N_d = 78.9 \times 10^3 \text{ cm}^{-3}$

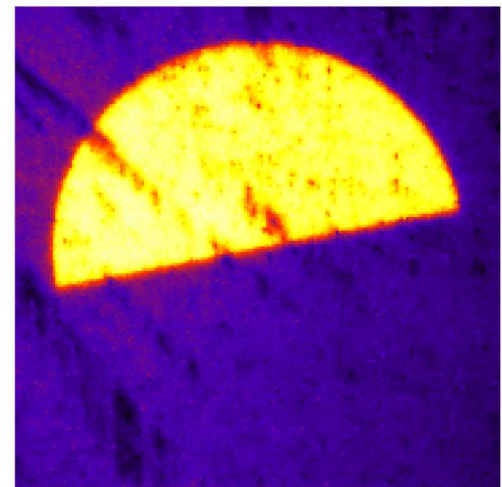
$\text{MOR}_{543} = 4.13 \text{ m}$   
 $\text{LWC} = 0.77 \text{ g/m}^3$   
 $N_d = 106.7 \times 10^3 \text{ cm}^{-3}$

Meteorological parameters derived from droplet distribution

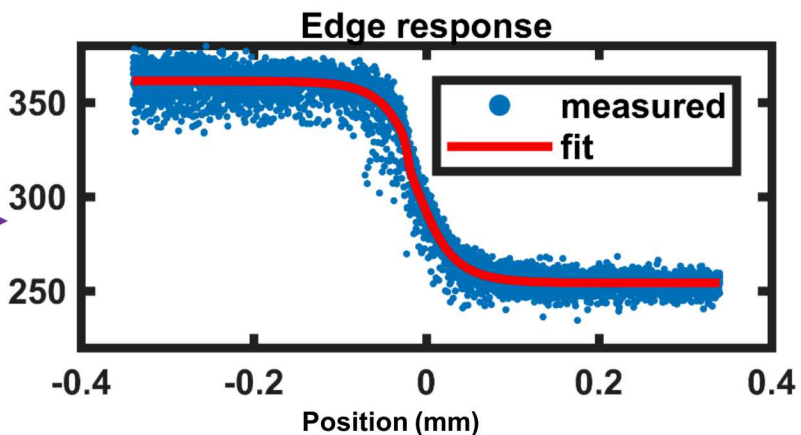
Brian J. Redman, et al., "Measuring resolution degradation of long-wavelength infrared imagery in fog," Opt. Eng. 58(5) 051806 (2019)

# Frequency measurement using edge response function

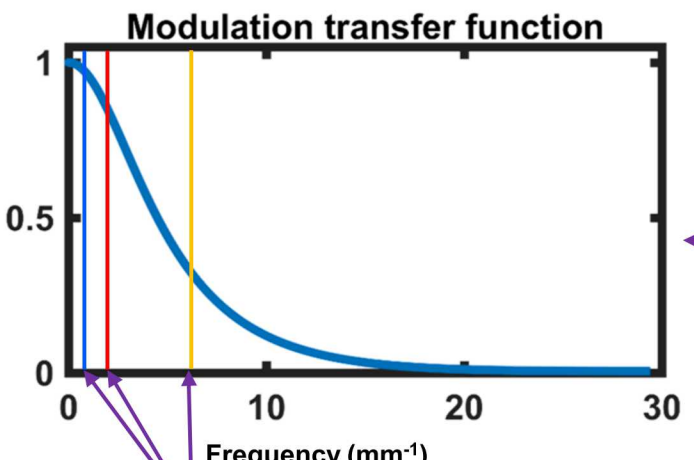
- MTF from edge response function
- Fitting edge
  - Sigmoidal functions
- Analytic derivative
  - doesn't amplify noise
- Line spread function
  - 1D projection of point spread function
- Fourier transform gives MTF
- MTF function of fog thickness
  - Three frequencies to display trends



Fit the edge response function

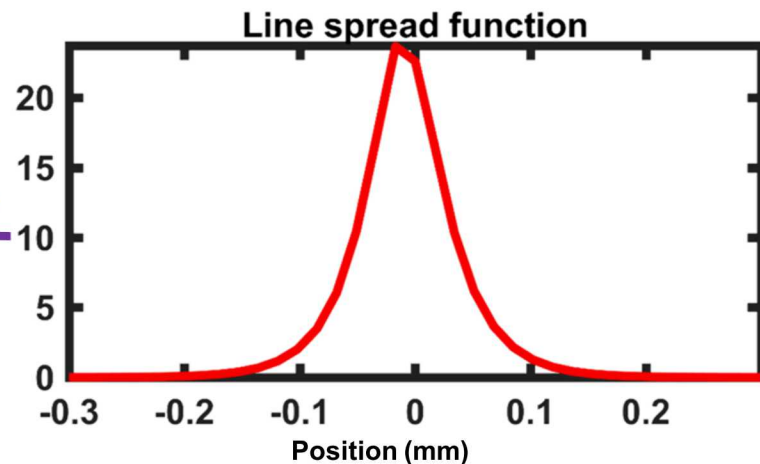


Analytic derivative from fitting coefficients

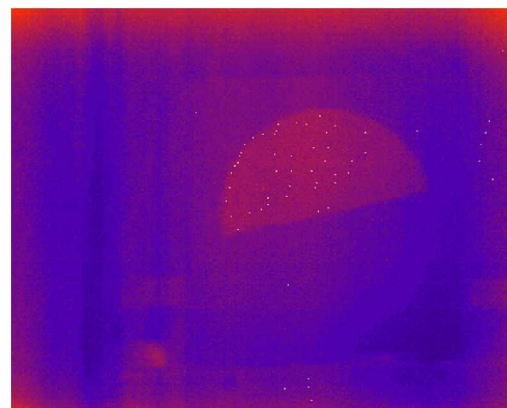


Fourier transform

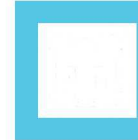
Example frequencies selected for display



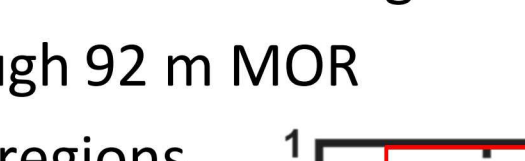
# Measurements synced across instruments

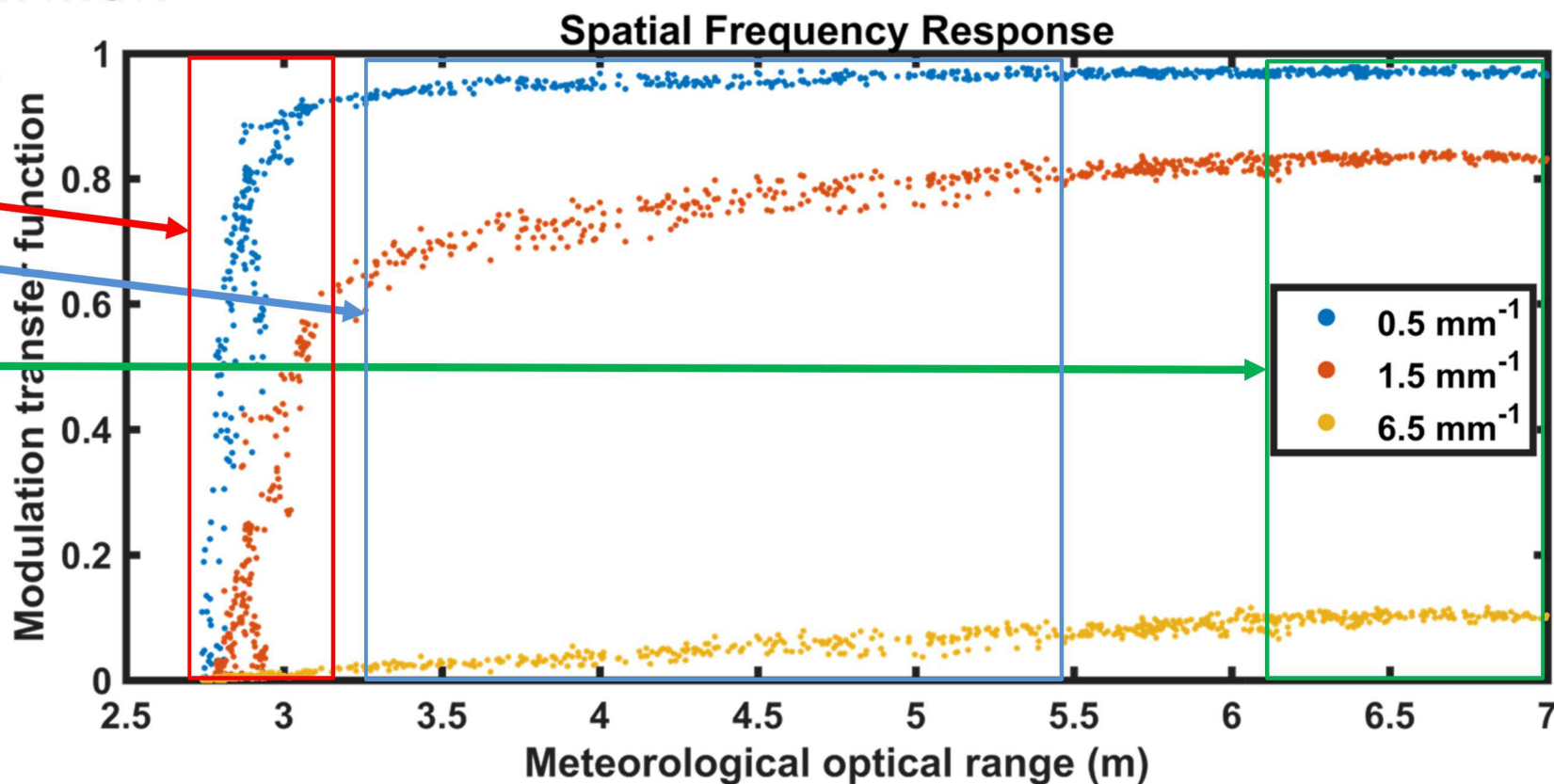


# Frequency response dependent on fog thickness



- Example frequencies of the MTF vs. fog thickness
- Effective distance through 92 m MOR
- Frequency response in regions
  - Noise floor
  - Frequency recovery
    - Slope frequency dependent
  - Steady state



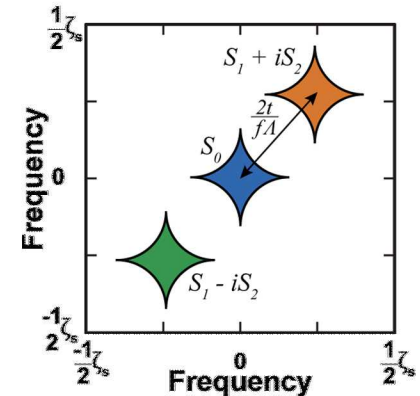
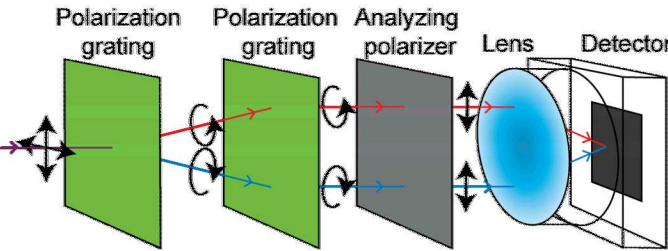


# Modeling and measurements of Four optical systems

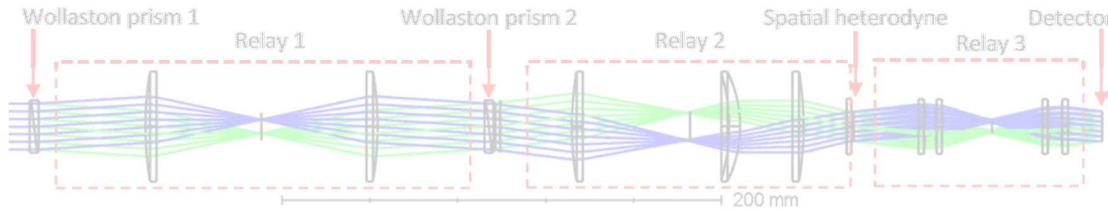
## 1. Long-wave infrared measurement of image degradation caused by fog



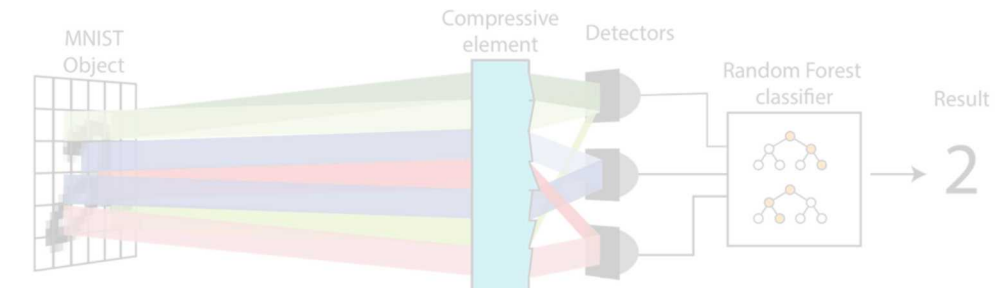
## 2. Channeled imaging polarimeter



## 3. Long-wave infrared snapshot Fourier transform spectrometer

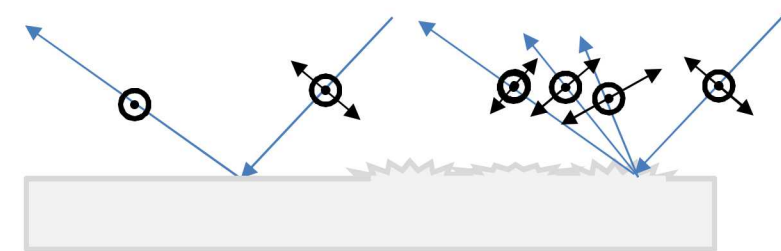


## 4. Compressive classification





- Polarization gives information about surfaces
- Stokes polarimeter
  - Linear Stokes
- Snapshot polarimeters
  - High temporal resolution, decreased spatial resolution
  - Modulated irradiance
    - Simpler fabrication

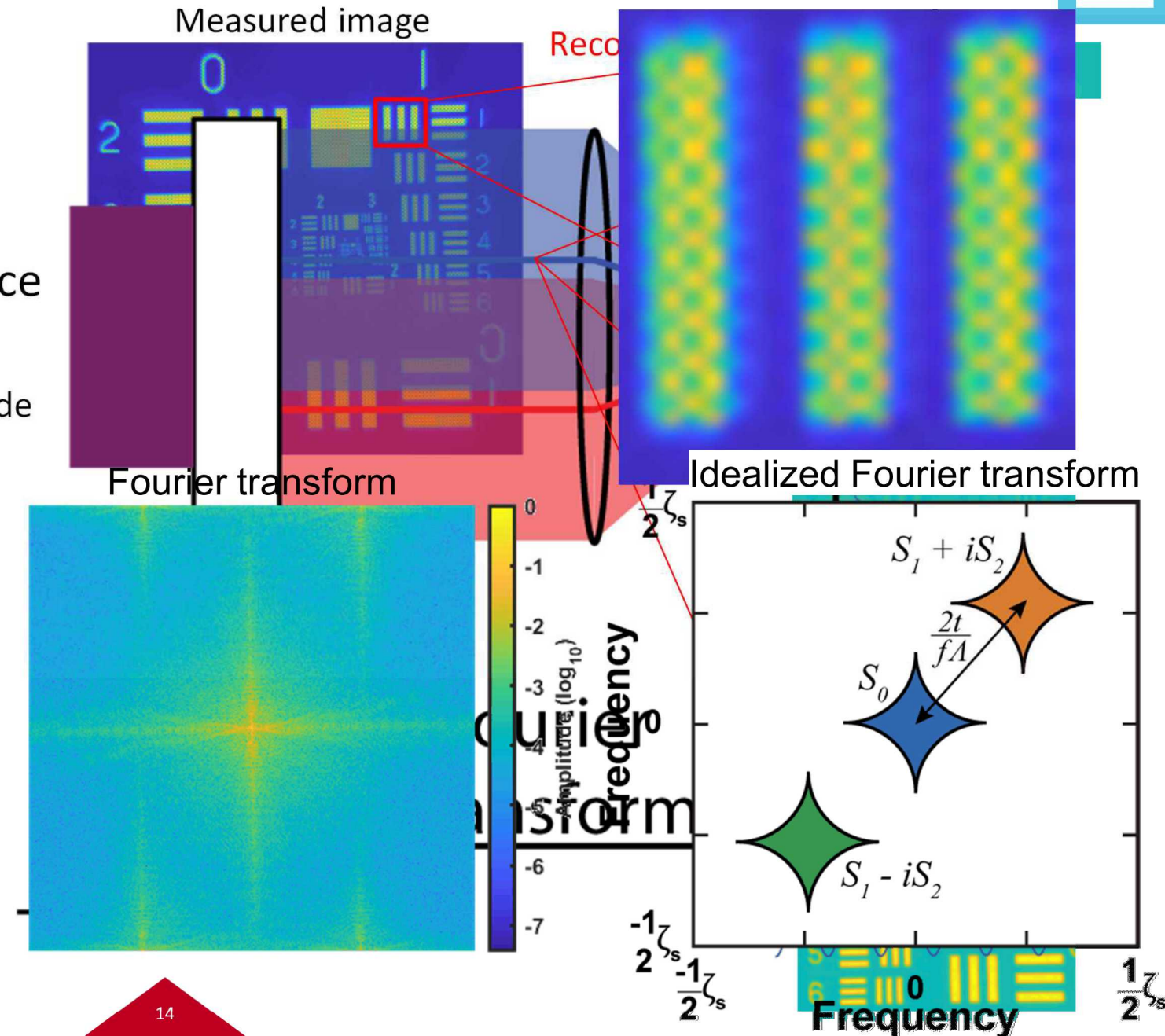


Stokes parameters

$$\mathbf{S} = \begin{bmatrix} S_0 \\ S_1 \\ S_2 \\ S_3 \end{bmatrix} = \begin{bmatrix} \Phi_{\text{total}} \\ \Phi_{\leftrightarrow} - \Phi_{\uparrow\downarrow} \\ \Phi_{\nearrow} - \Phi_{\nwarrow} \\ \Phi_{\text{U}} - \Phi_{\text{O}} \end{bmatrix}$$

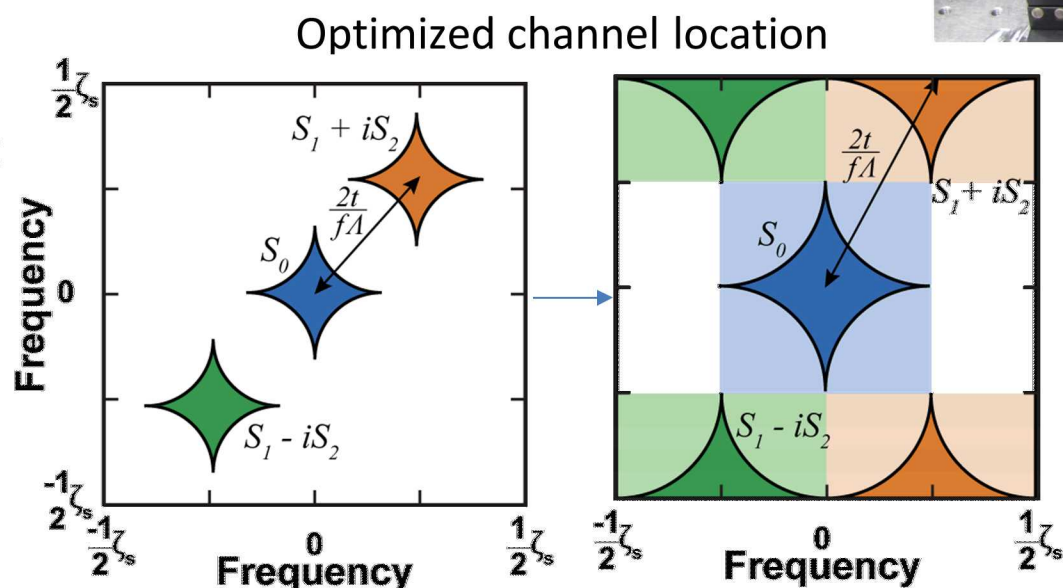
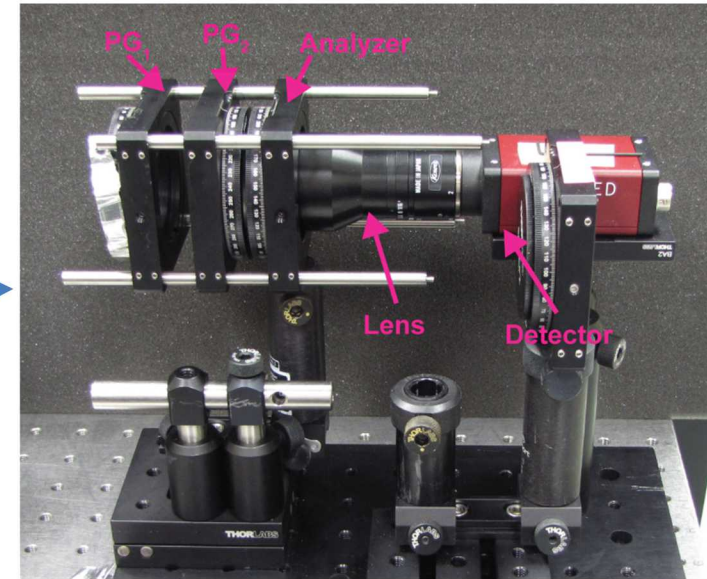
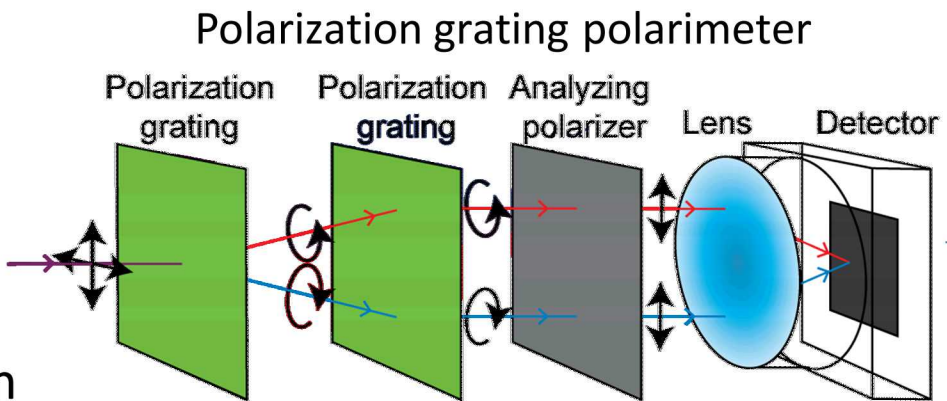
# Interference to encode information into Fourier domain

- Channeled optical systems
- Shear creates modulated irradiance
  - Visibility
    - Signal strength dependent on amplitude of modulation
- Images separated in Fourier domain
  - Channels



# Polarization grating polarimeter optimized for maximum resolution

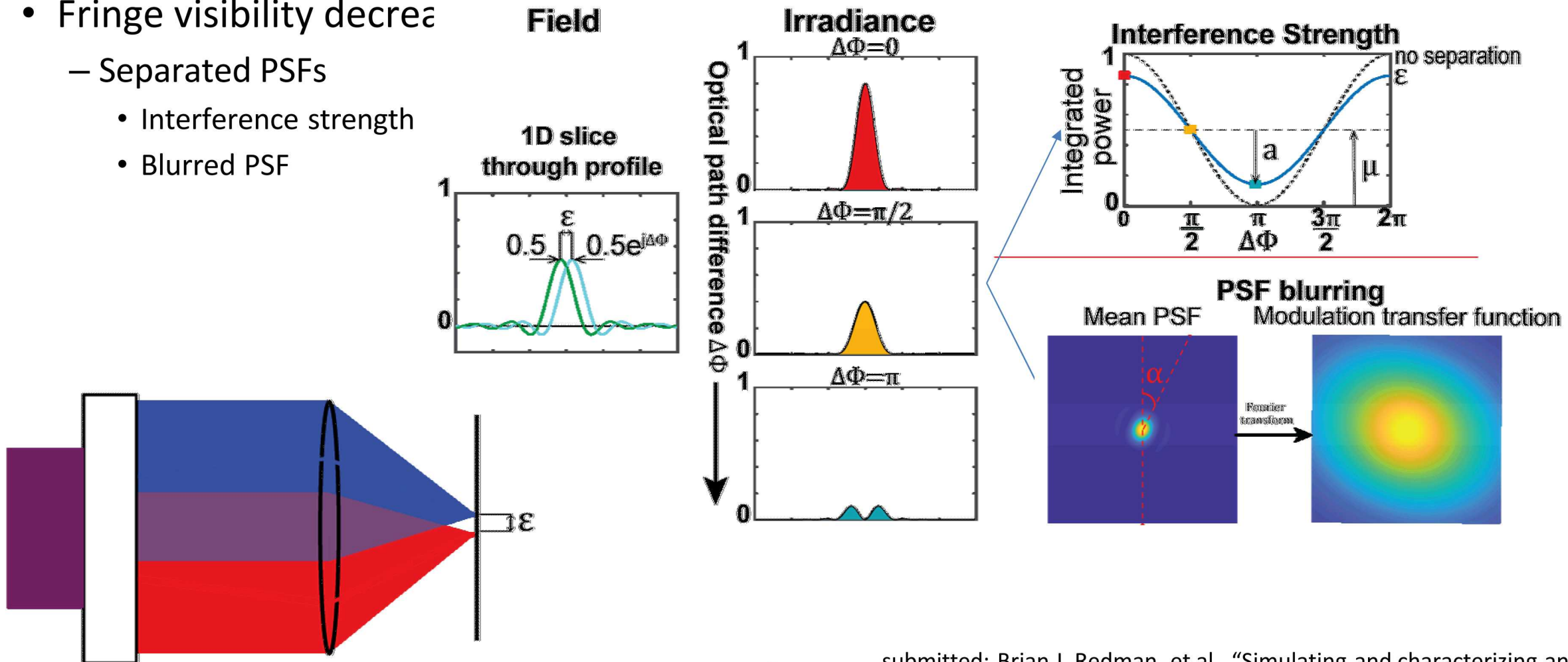
- Polarization gratings create shear
  - Diffraction grating
  - Polarization order selection
- Separation and angle set channel location
- Physical instrument created to test performance



submitted: Brian J. Redman, et al., "Simulating and characterizing an optimized snapshot channeled imaging polarimeter," Optics Express

# Decreased modulation amplitude due to misalignment

- Fringe visibility decreases
  - Separated PSFs
    - Interference strength
    - Blurred PSF

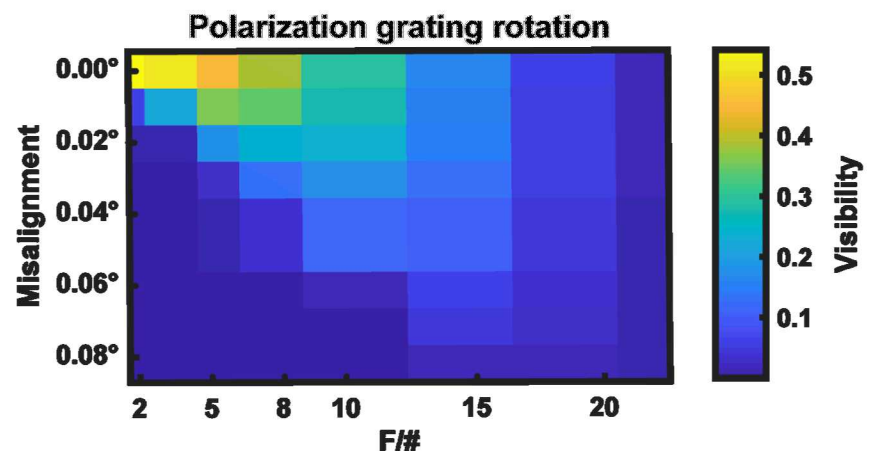
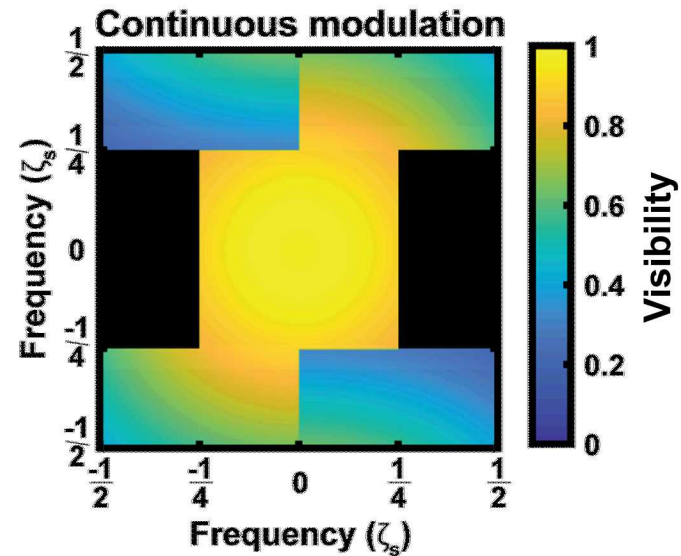
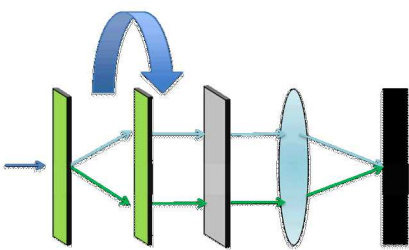


submitted: Brian J. Redman, et al., "Simulating and characterizing an optimized snapshot channeled imaging polarimeter," Optics Express

# Performance of polarimeter is limited by component alignment and pixel sampling

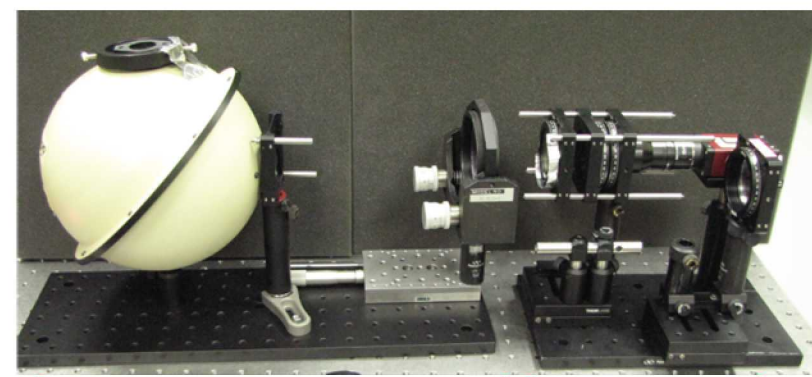


- Pixel sampling
  - Sinc MTF
  - Modulated channels
    - High spatial frequencies
  - Fundamental limit of system
- Component misalignment
  - PSF separation and Pixel MTF
  - Highly sensitive
  - Width of PSF matters



submitted: Brian J. Redman, et al., "Simulating and characterizing an optimized snapshot channeled imaging polarimeter," Optics Express

# Performance of channeled polarimeter measured with resolution target

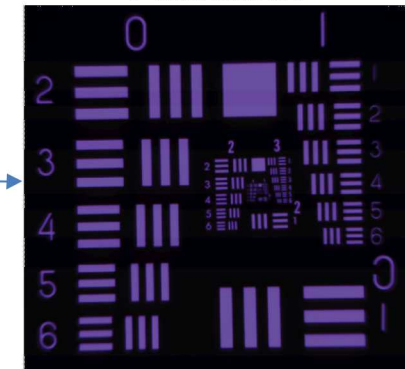


Test bench

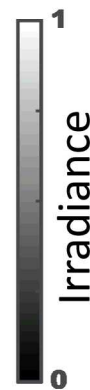
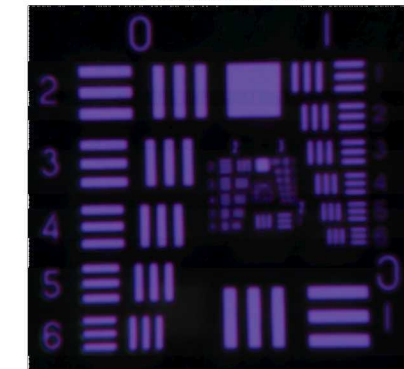


Polarization Grating Polarimeter

Rotating Polarizer  
Polarimeter

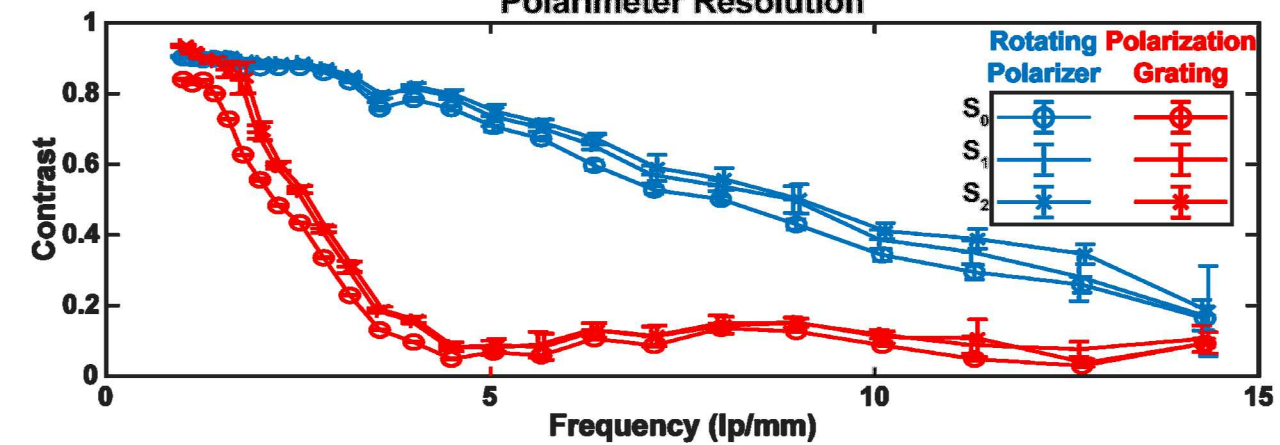


Polarization Grating  
Polarimeter



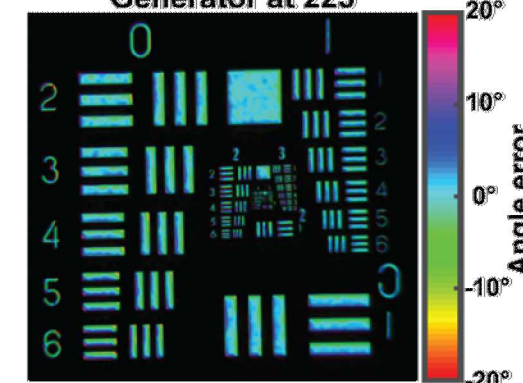
Resolution measurement

Polarimeter Resolution



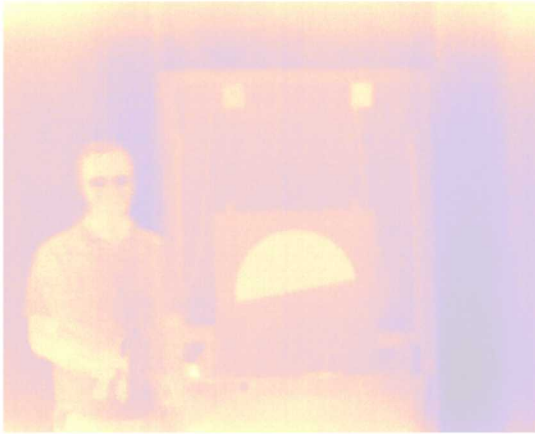
Angle measurement

Generator at 225°

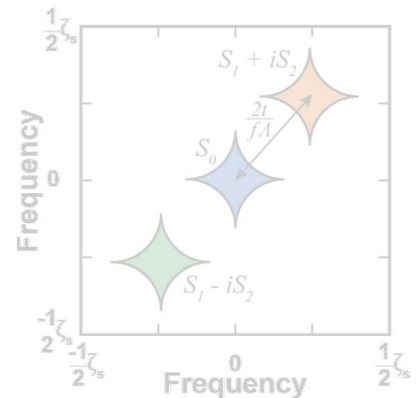
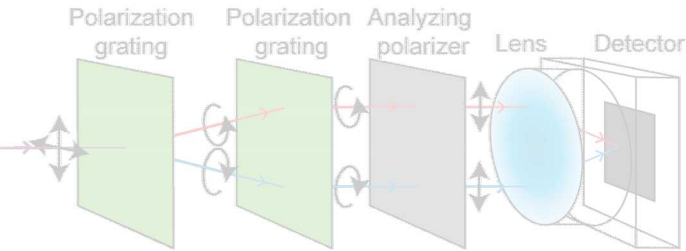




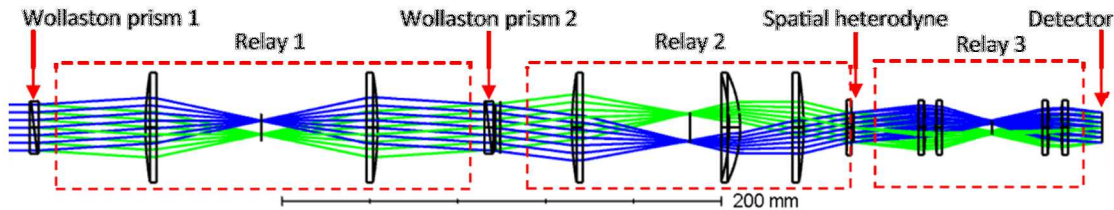
## 1. Long-wave infrared measurement of image degradation caused by fog



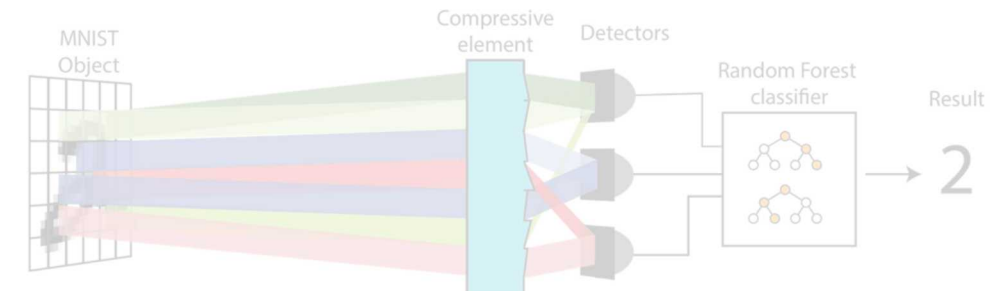
## 2. Channeled imaging polarimeter



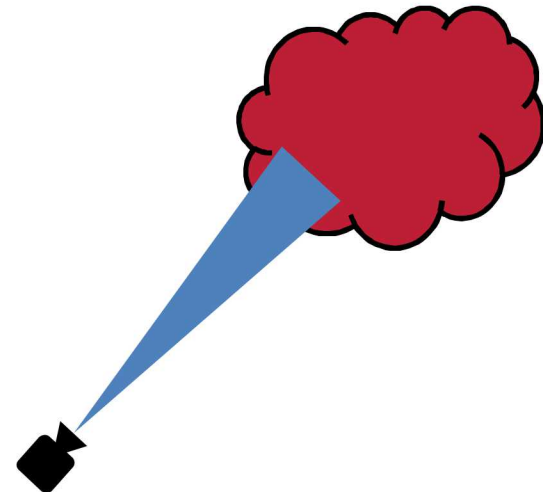
## 3. Long-wave infrared snapshot Fourier transform spectrometer



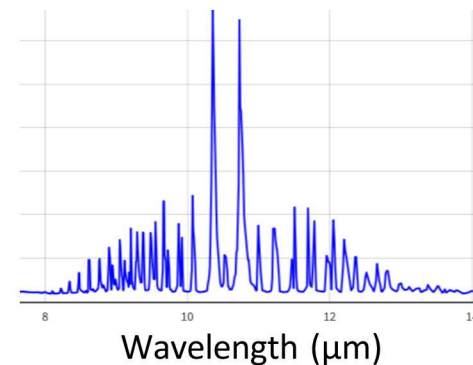
## 4. Compressive classification



- Non-imaging gas detection
- Spectral measurements
  - Enable material identification
  - Detection can be more important than localization
  - Instrument point and field of view
- LWIR enables passive measurements

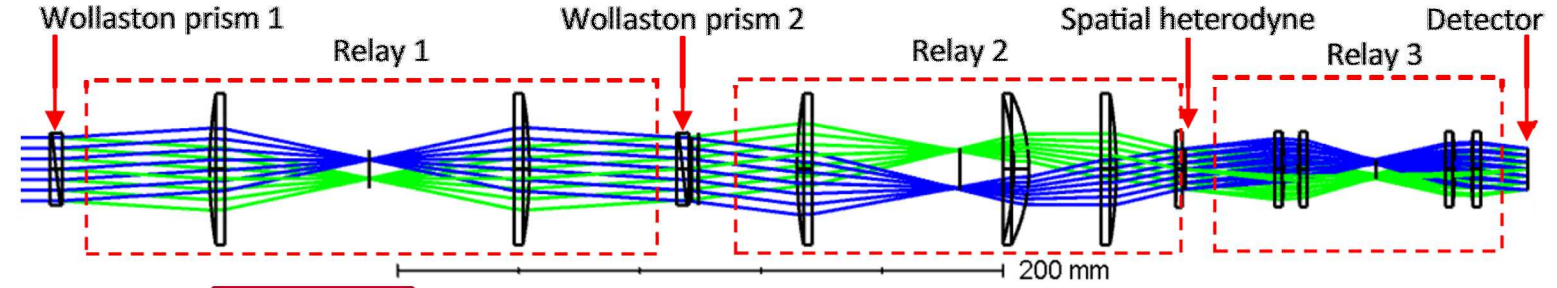
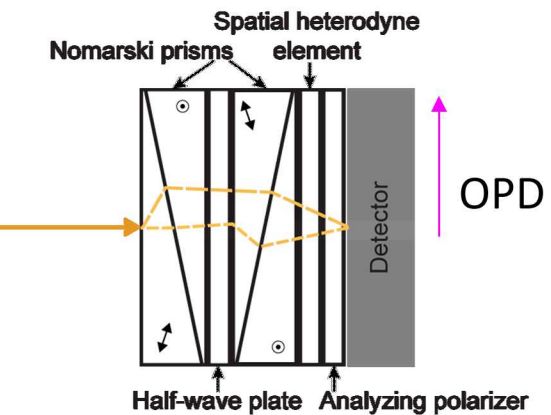
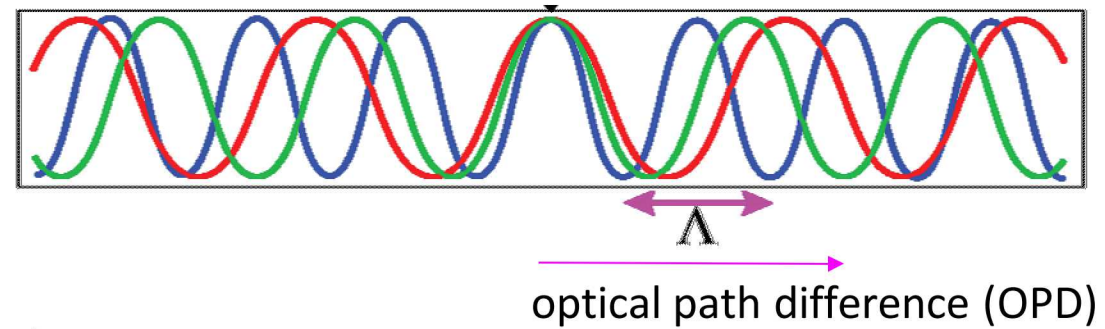


Spectral measurement



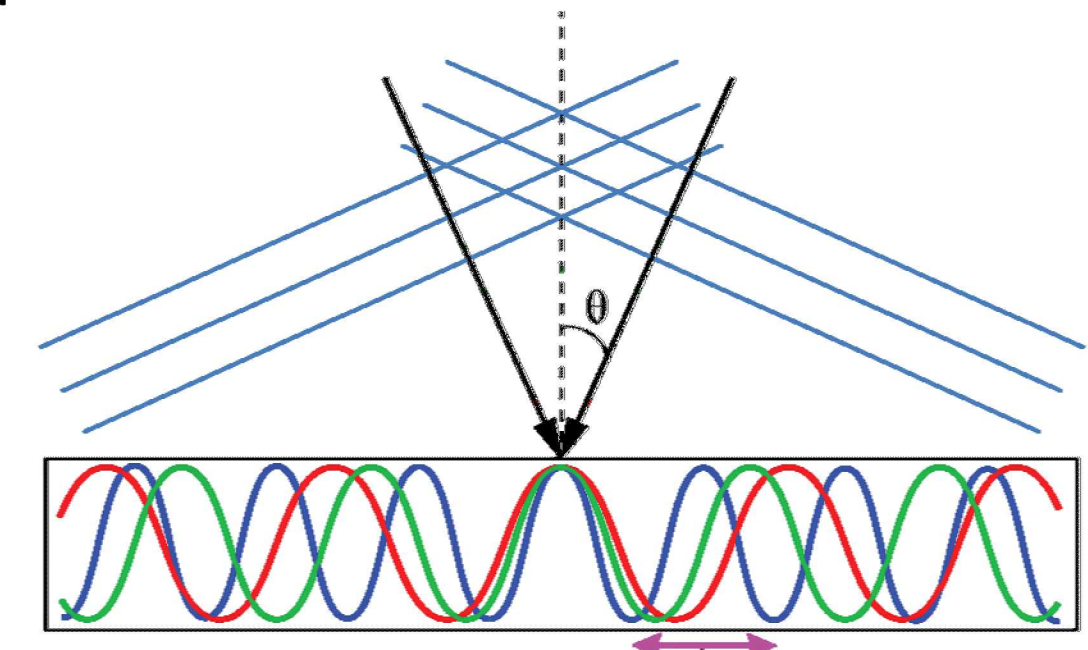
# Fourier transform spectrometers (FTS) encode spectra into Fourier domain

- Interference creates a weighted sum of sinusoids
  - Fourier transform
- Can be implemented as a solid state device
  - Enables hand held instrument
  - Bonded together
  - Demonstrated in the visible
- LWIR implementation more risky
  - Birefringent materials rare
  - Expanded design for proof of concept



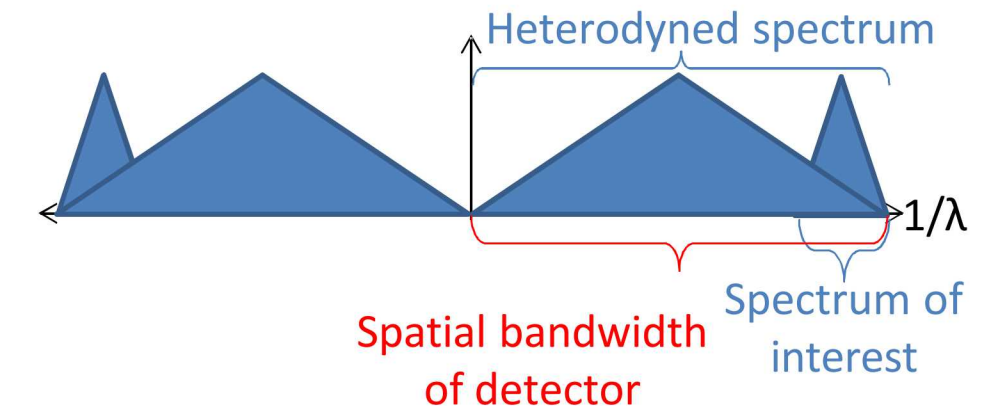
# Spatial heterodyne

- Two polychromatic plane waves
  - Frequency from 0 to max frequency
  - Low resolution after Fourier transform
- Spatial heterodyne
  - Shift the spectrum lower
  - Can use spatial bandwidth of detector
- Wavelength dependence to incident angle
  - Diffractive optic



$$\Delta = \frac{2\pi}{|\Delta k|} \approx \frac{2\pi}{\frac{2\pi}{\lambda} \sin(\theta)} \left( \frac{\lambda}{2 \sin(\theta)} \left( \frac{m\lambda}{d} \right) \right)$$

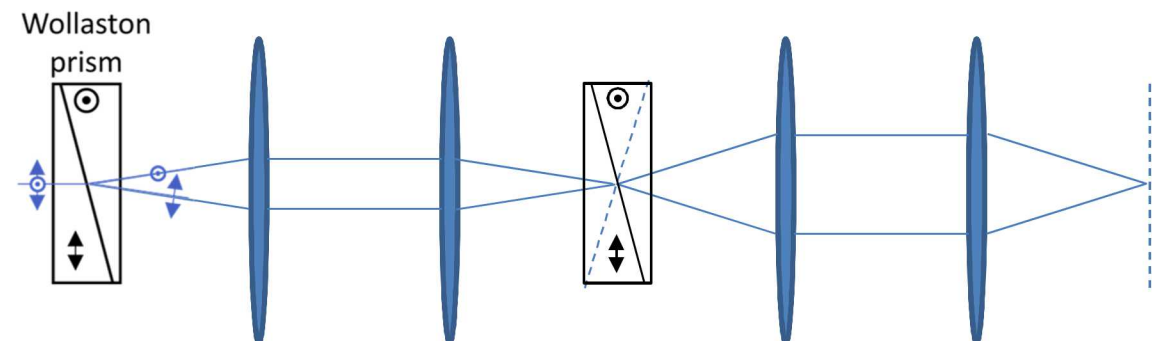
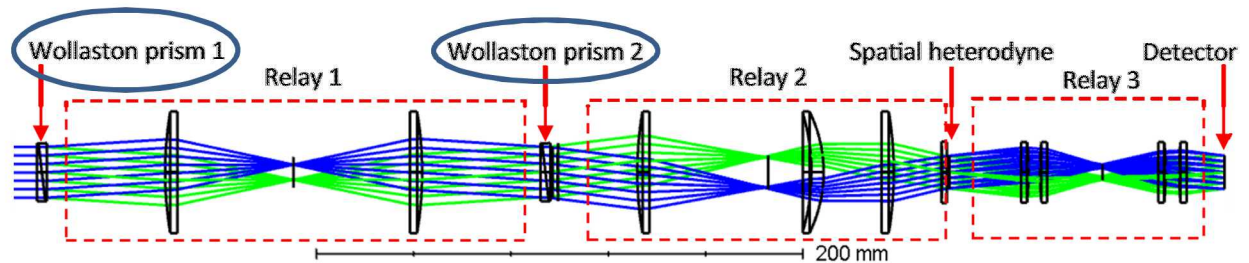
Fourier transform of interferogram



# Many separate elements as proof of concept for solid state Nomarski design



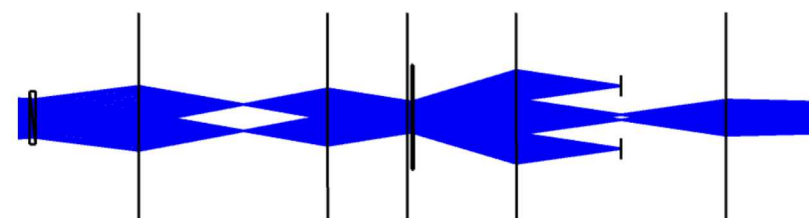
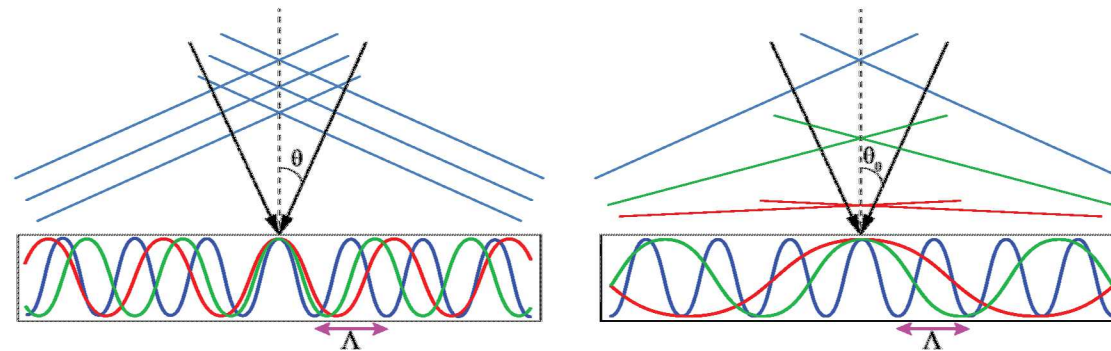
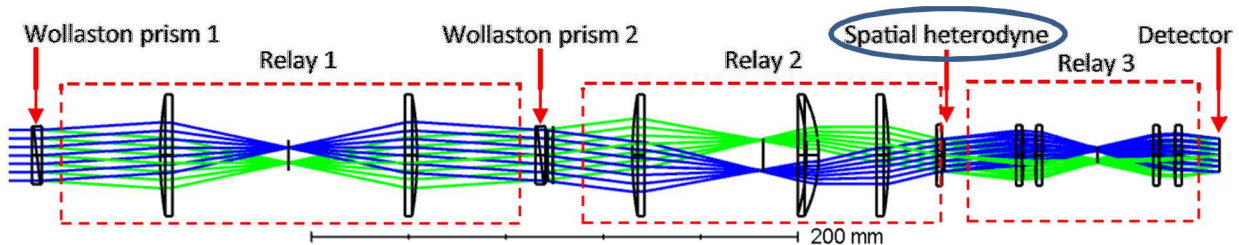
- Wollaston prism
  - Splits light
  - Slanted interference plane
- Second prism
  - Doubles angle
  - Flattens interference plane



# Many separate elements as proof of concept for solid state Nomarski design



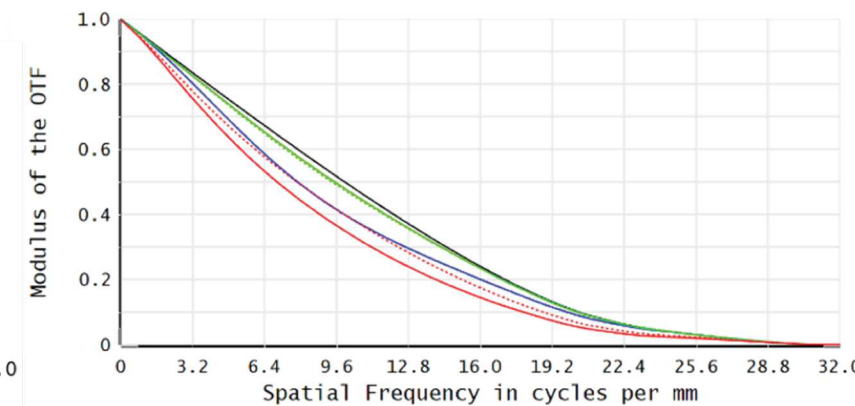
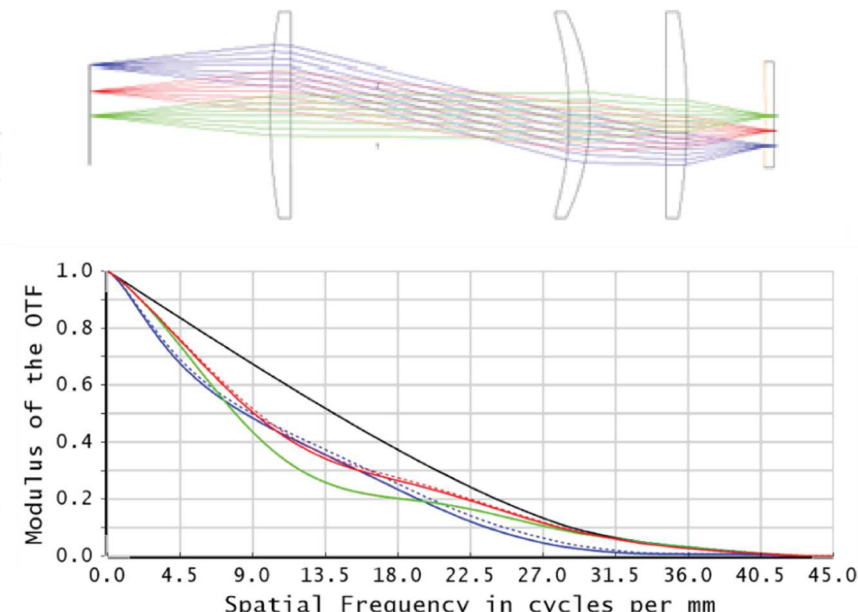
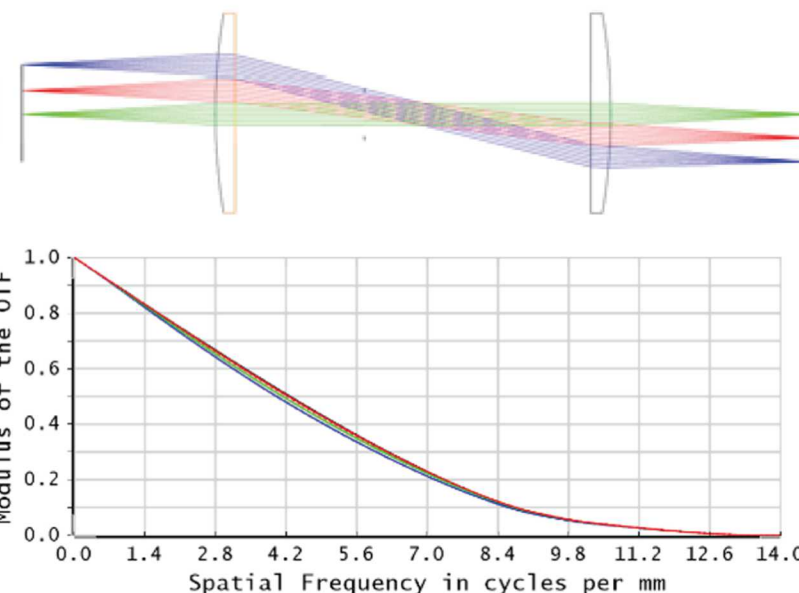
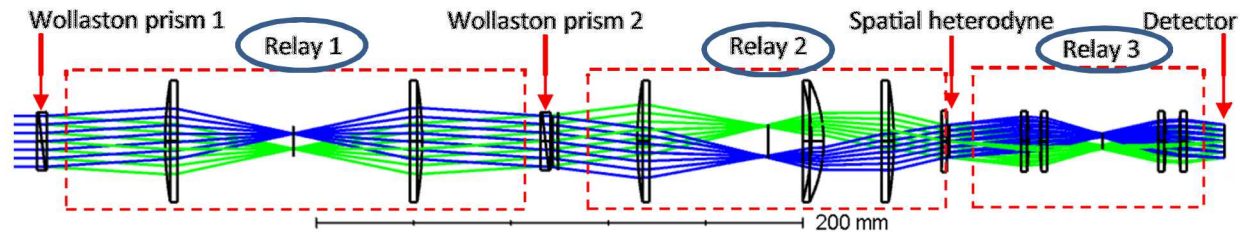
- Spatial heterodyning
  - Reduce spatial frequency
- Diffractive optic
  - Change angle of plane waves
  - Fourier filter to remove unwanted orders



# Many separate elements as proof of concept for solid state Nomarski design



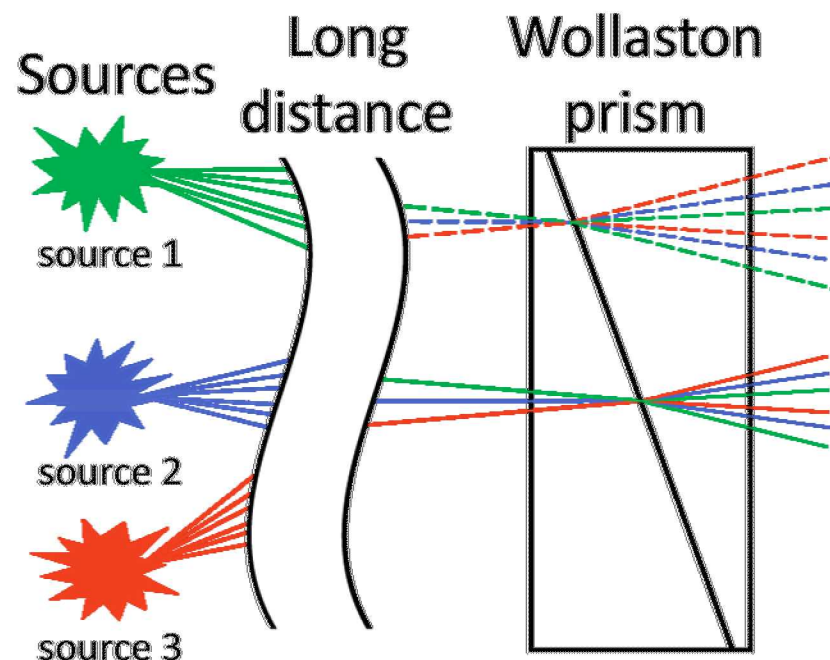
- Relays
  - Image interference plane
  - Optimized in sections
- Telecentric
  - Ray cone represents split angle



# Pitfall of modeling the Fourier transform spectrometer



- Coherence
  - Crucial for simulations
  - MTF assumes coherent points

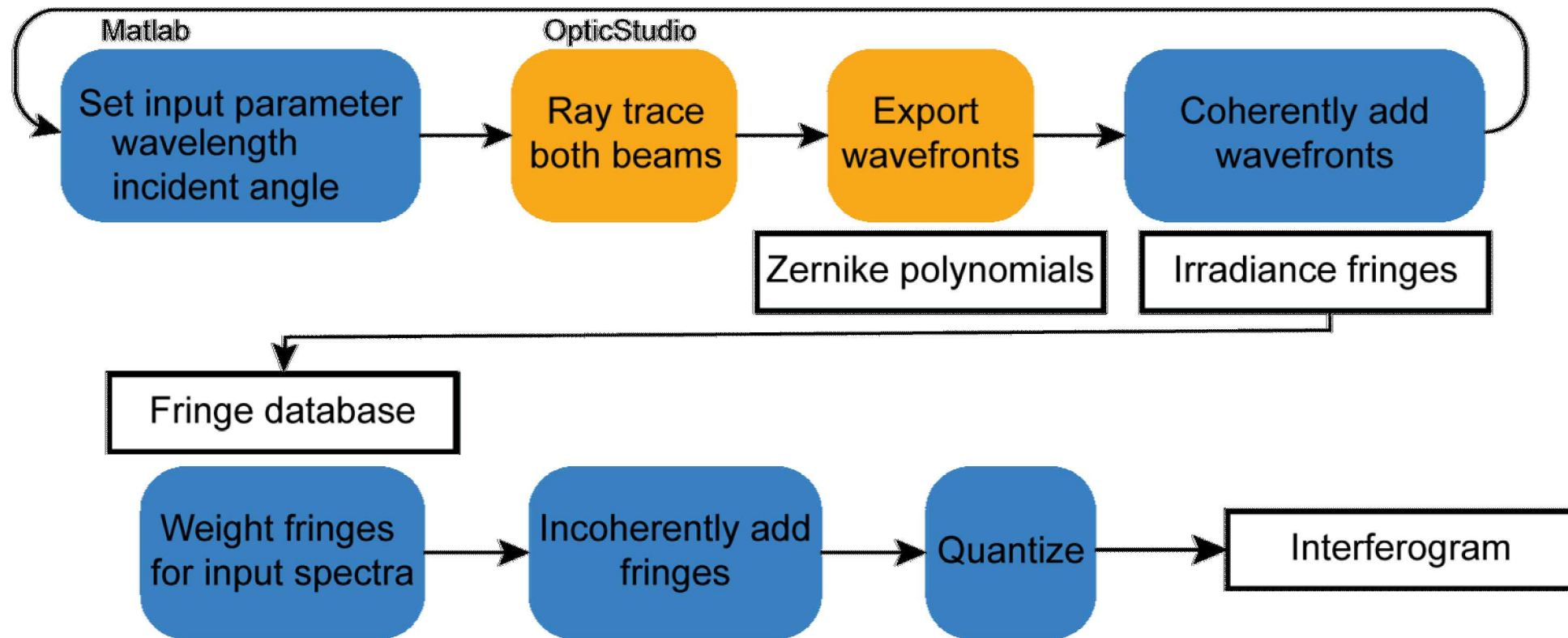


# Coherence directly controlled to remove assumptions



- Ray tracing efficient to estimate wavefronts
- Matlab to combine wavefronts

- Coherently
  - Split beams
- Incoherently
  - Input angles
  - Wavelengths

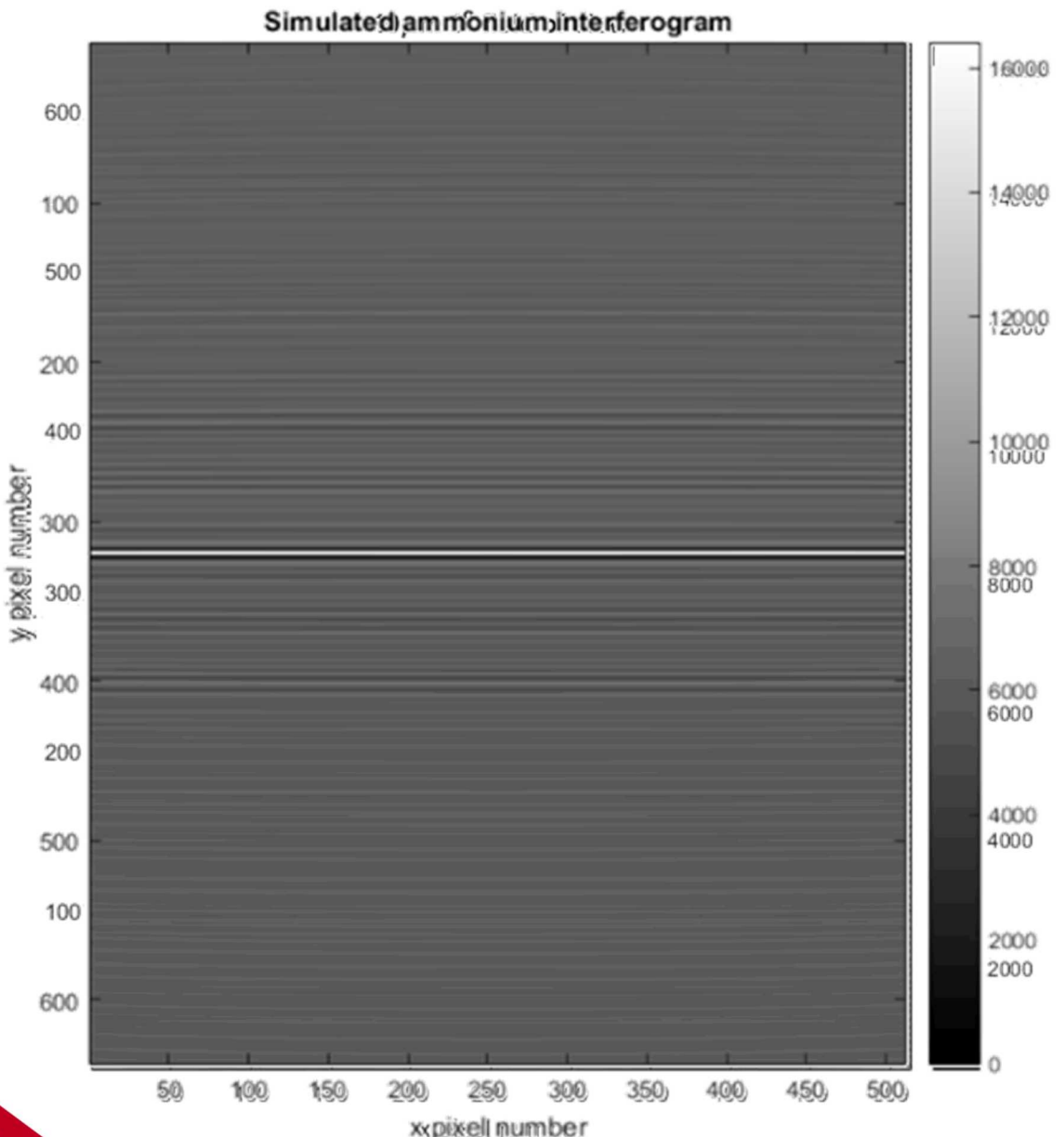
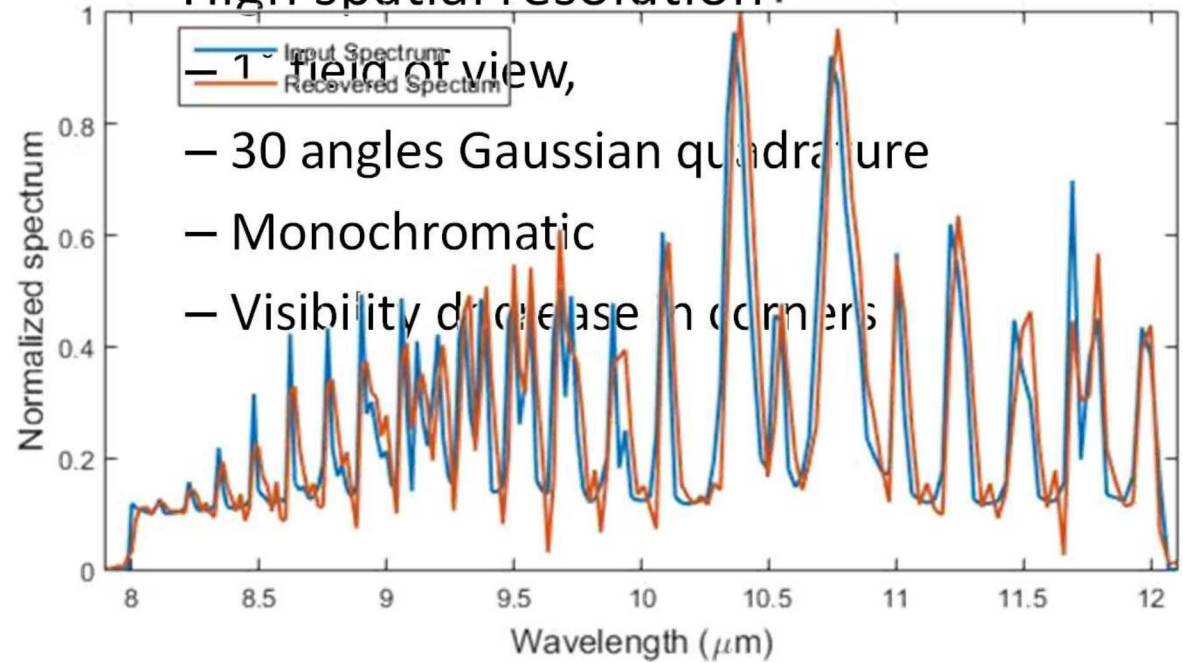


# Simulation models both spatial and temporal incoherence



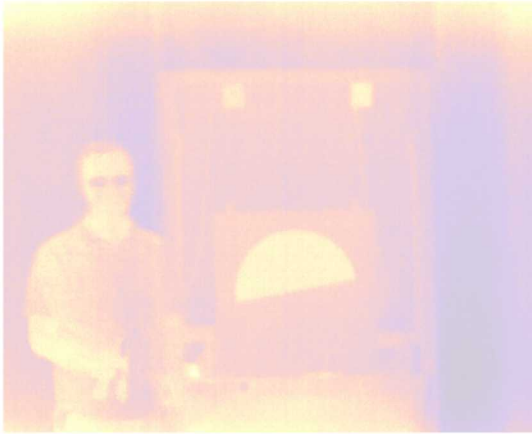
- High Spectral sampling
  - 400 wavelengths
  - $1^\circ$  field of view 7 angles
  - Reconstructed

## Simulated Ammonia Spectrum

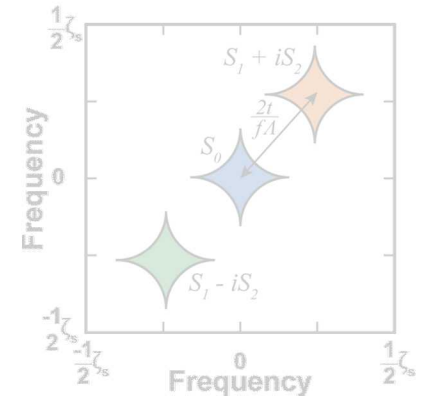
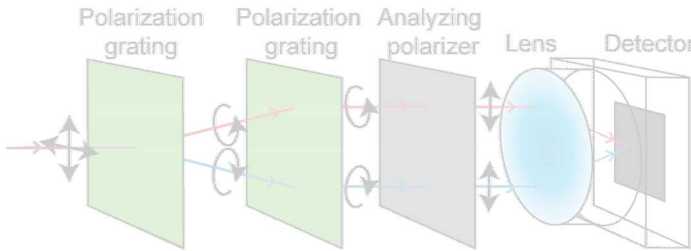




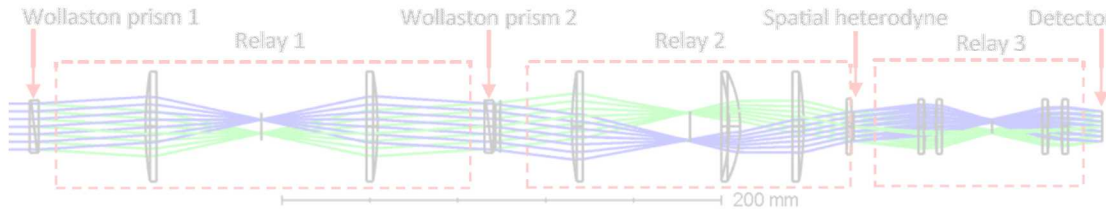
## 1. Long-wave infrared measurement of image degradation caused by fog



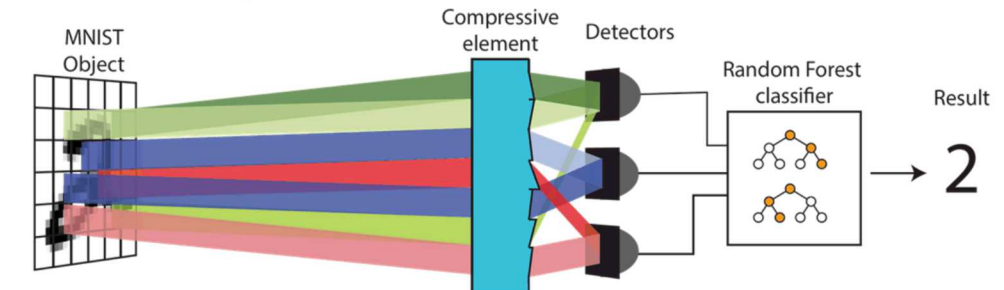
## 2. Channeled imaging polarimeter



## 3. Long-wave infrared snapshot Fourier transform spectrometer



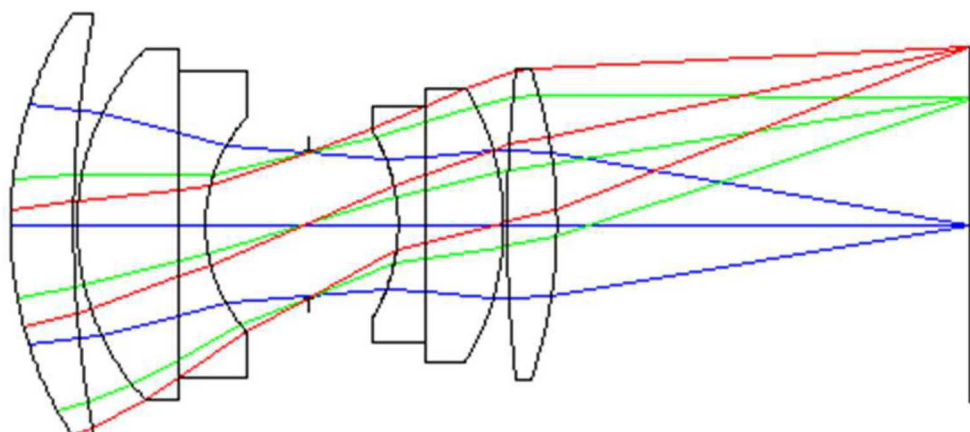
## 4. Compressive classification



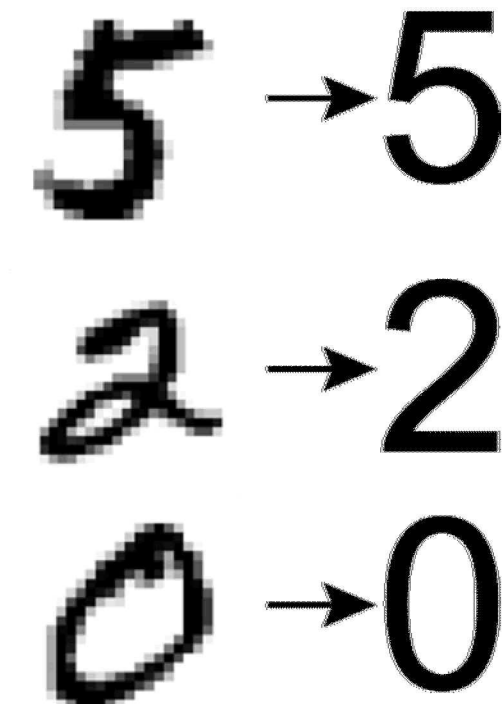
# Spatial resolution not required for detection



- Classification requires small subset of scene
  - Final data product class not image
  - Image processing commonly compresses high resolution images
- Imaging over constrains
  - 1:1 mapping
  - Many element optical system
- Potential to reduce size weight and power

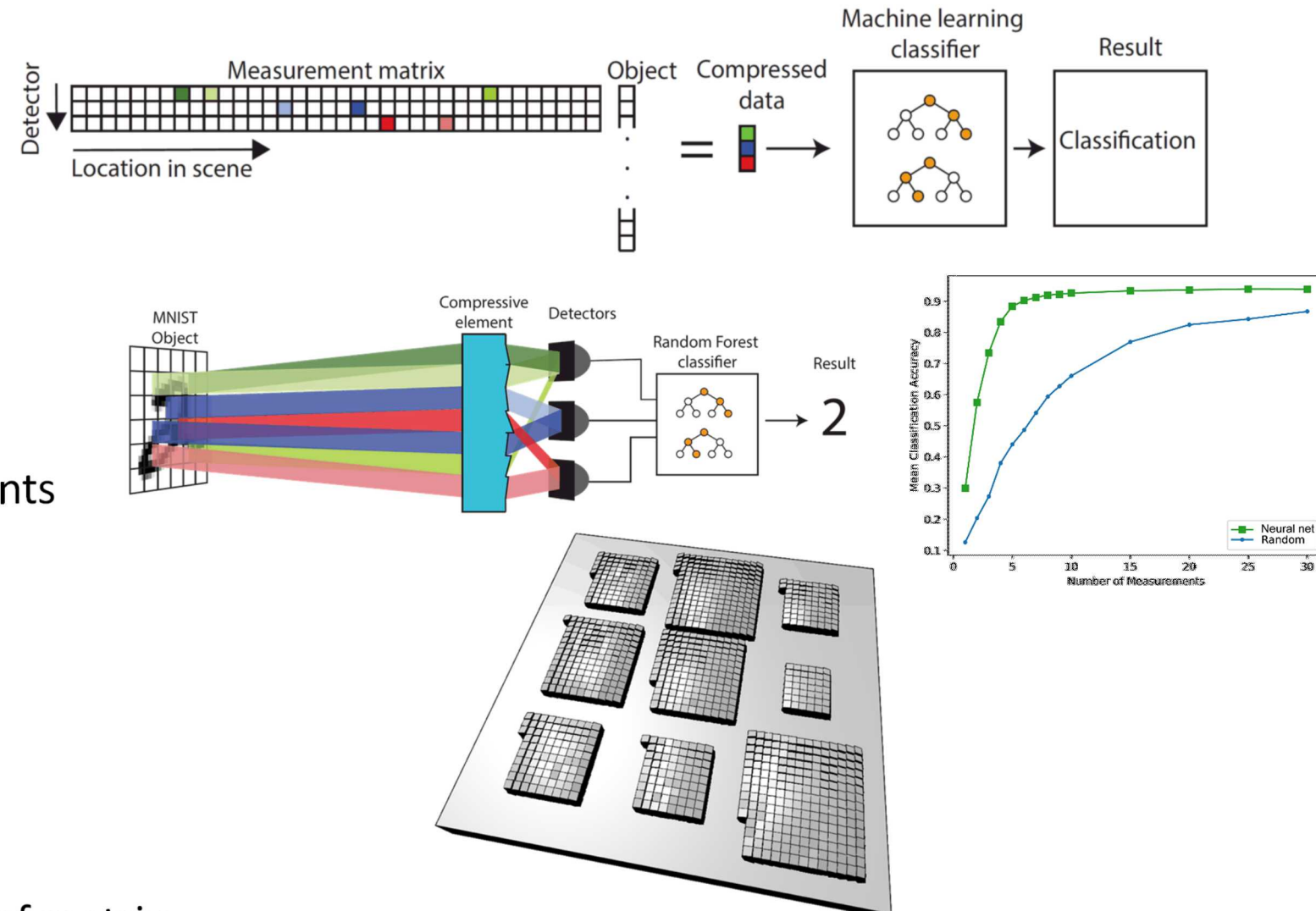


MNIST dataset



# Compressive classification

- Classification algorithms compress images
  - Reduce size of dataset
    - 784  $\rightarrow$  9 for MNIST
  - Remove information that does not differentiate classes
  - Reduce computation requirements
- Hardware compression
  - Physical implementation of compression matrix
  - Requires multiple field angles mapped to each detector
- Prism array
  - Prism for Each non-zero entree of matrix

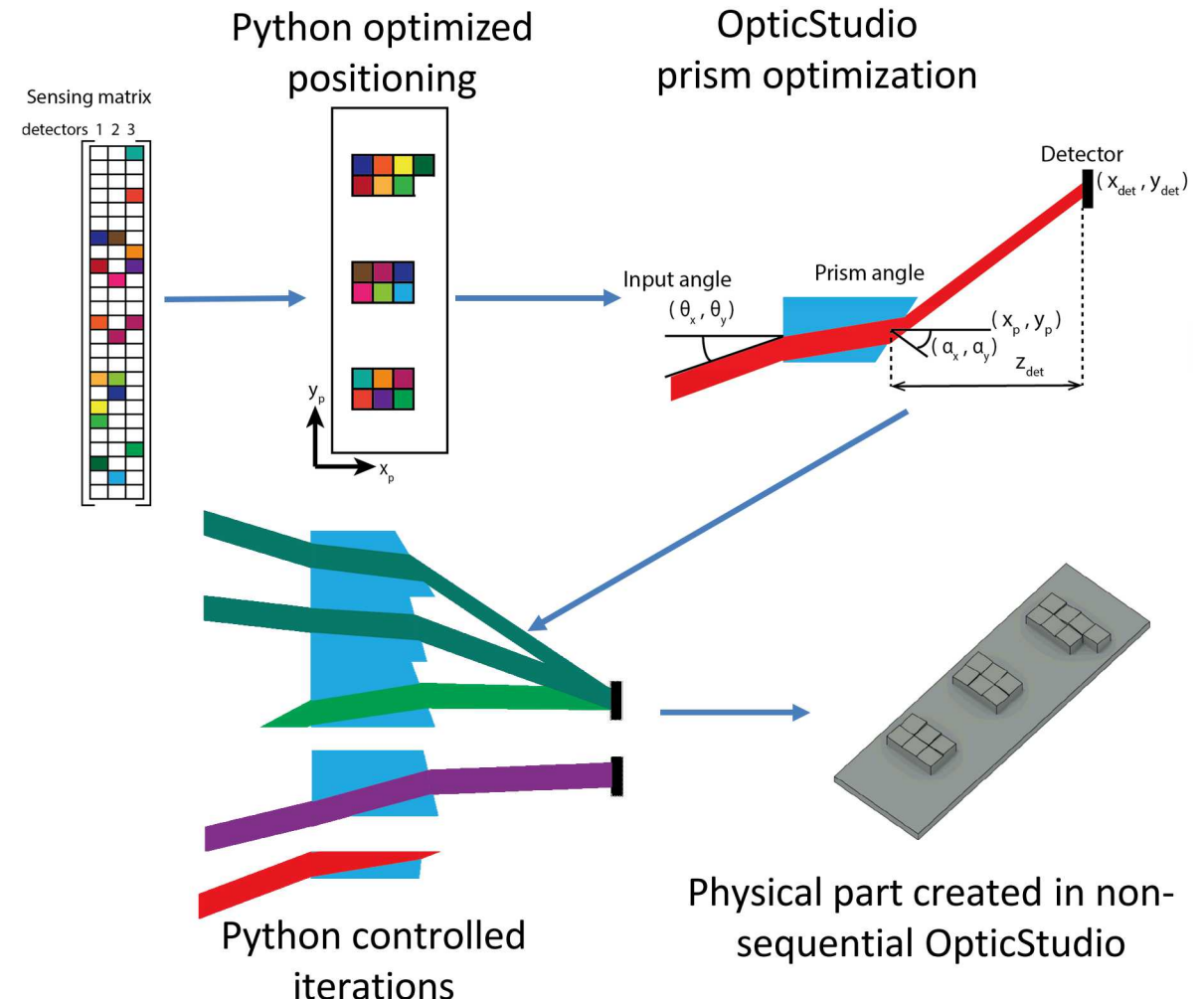
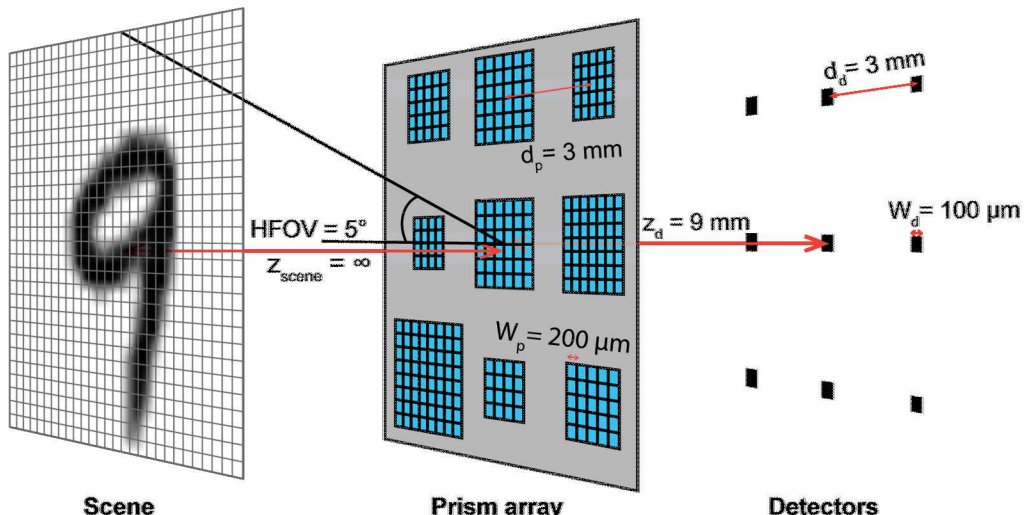


Submitted: B. J. Redman, et al., "Performance evaluation of two optical architectures for task-specific compressive classification," *Optical Engineering* 59(5), 2019.

# Autonomous workflow for realizing a mathematical construct



- Assign physical parameters to dataset
- Combination of Python and OpticStudio
- Workflow independent of dataset complexity

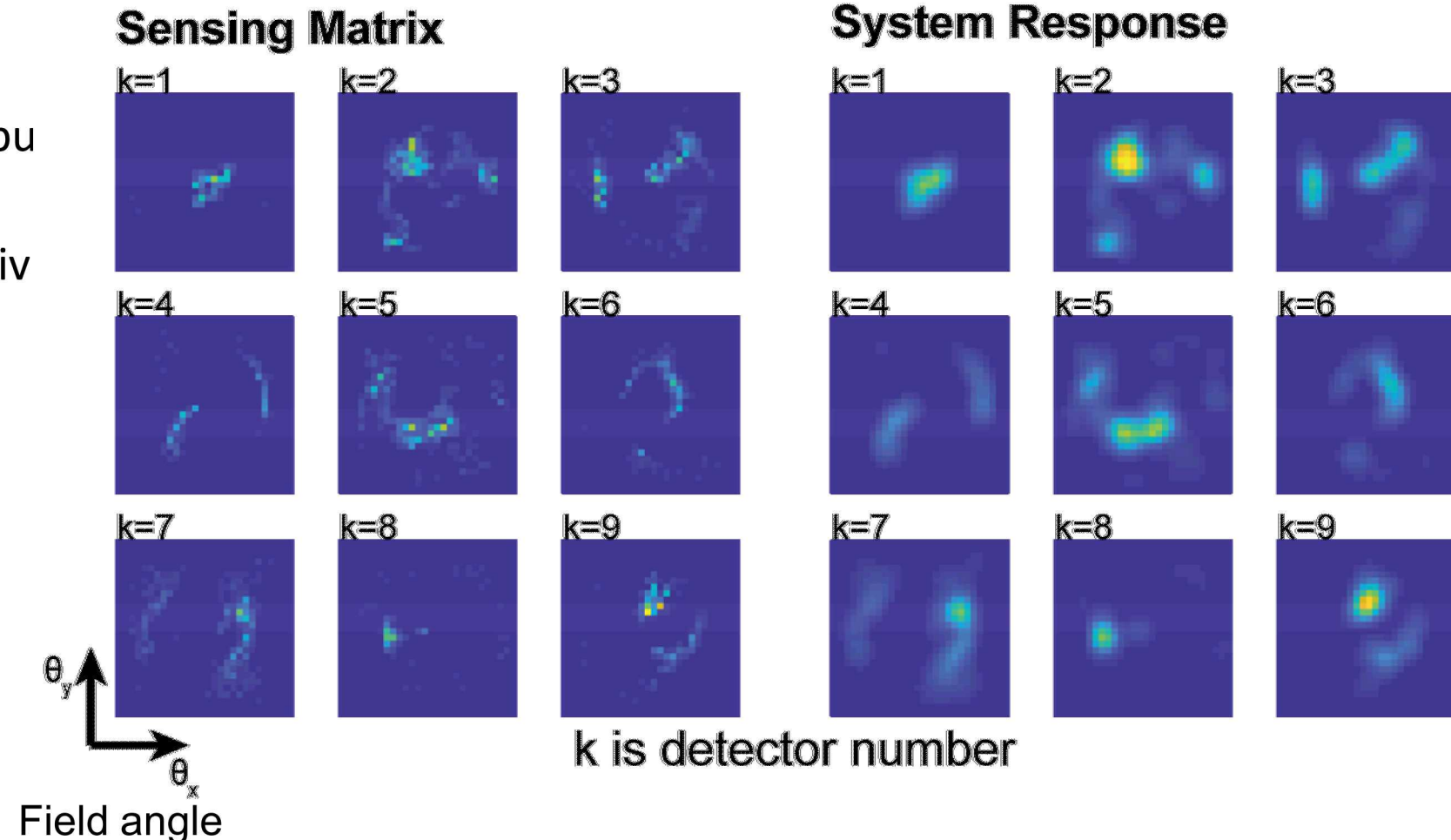


Minor revisions: B. J. Redman, et al., "Performance evaluation of two optical architectures for task-specific compressive classification," *Optical Engineering*, 2019.

# Physical realization of sensing matrix

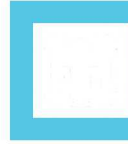


- Non-sequential ray trace
  - Separate trace for each input angle
  - Determine detector sensitivity
- Prism array
  - Blurring caused by prism accepting larger angle
- System response
  - Can be used to simulate performance

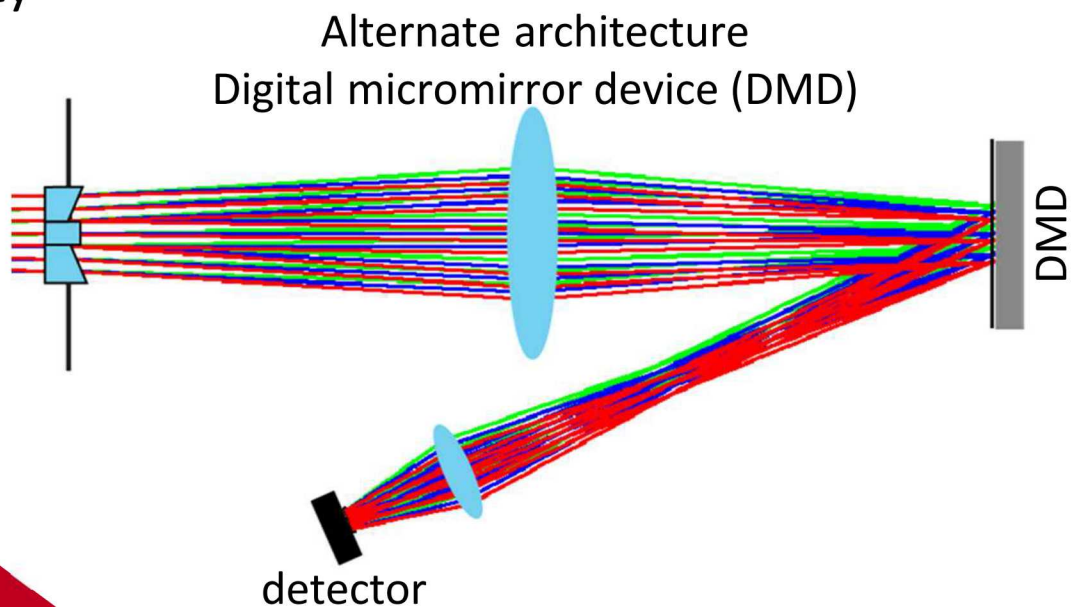
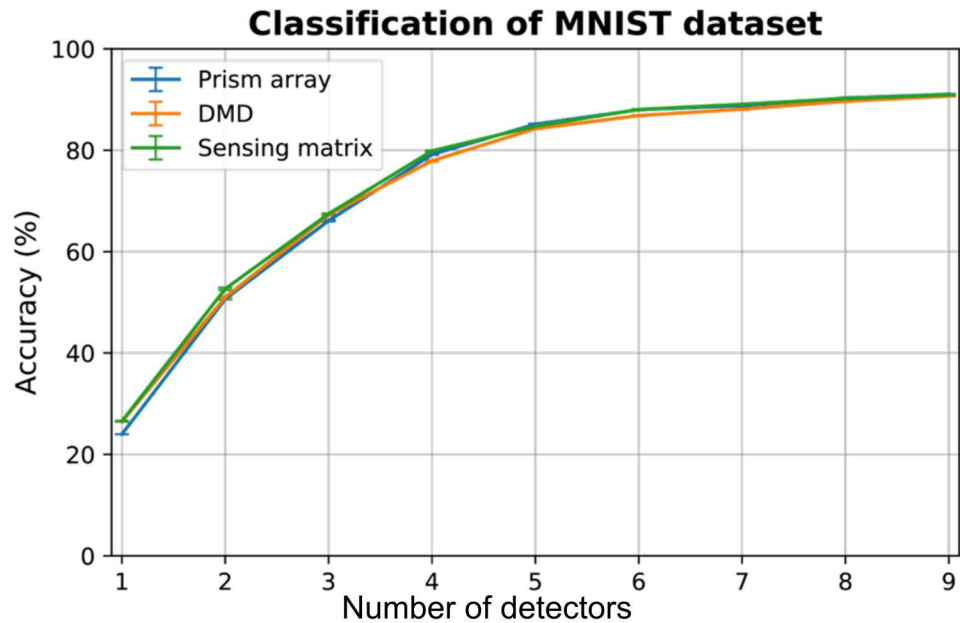
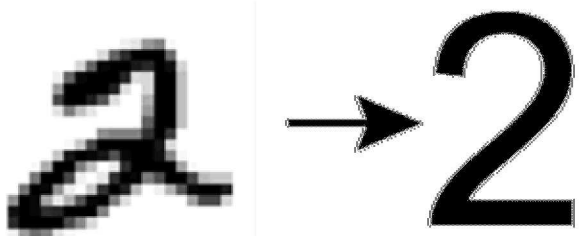


Minor revisions: B. J. Redman, et al., "Performance evaluation of two optical architectures for task-specific compressive classification," *Optical Engineering*, 2019.

# Simulations of classification accuracy to determine performance



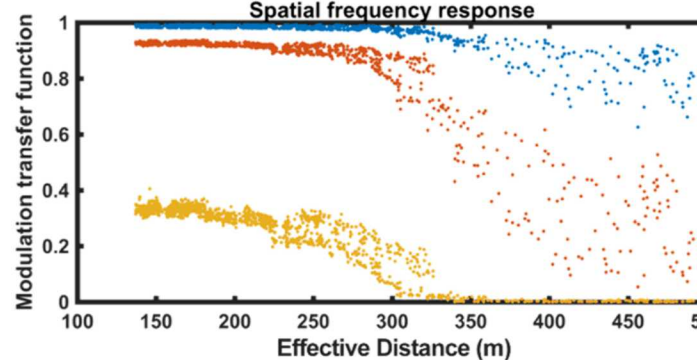
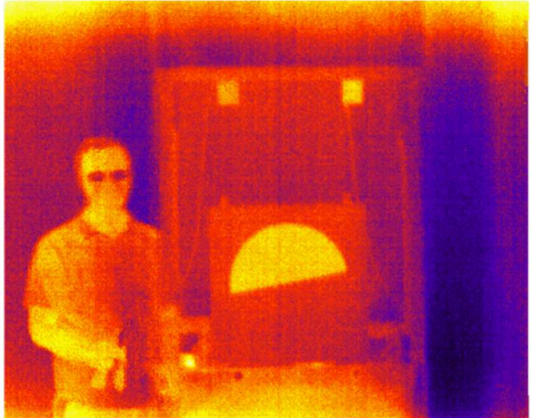
- Sensing matrix ideal performance
- Realized with two optical architectures
  - Prism array
  - Digital micromirror device (DMD)
- Simulation uses sensing matrices
  - Nonsequential ray trace to determine sensitivity
  - Used to compress MNIST images
  - Random forest classifier



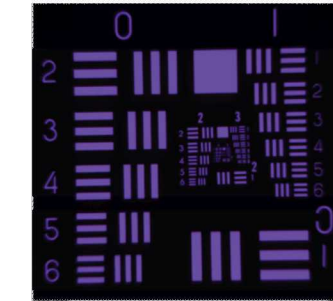
# Measurement and simulation of complex optical systems



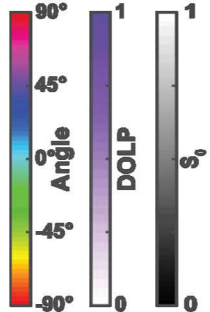
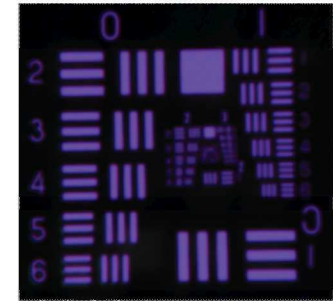
Target Distance = 16.76 m  
MOR = 6.85 m



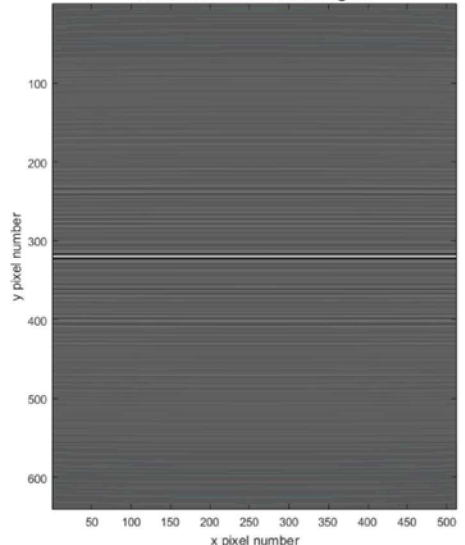
Rotating Polarizer  
Polarimeter



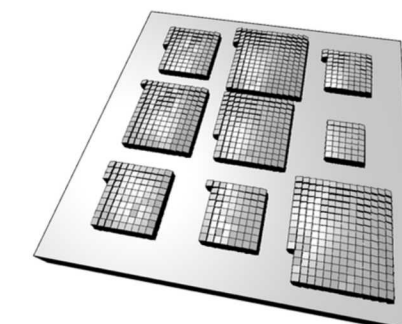
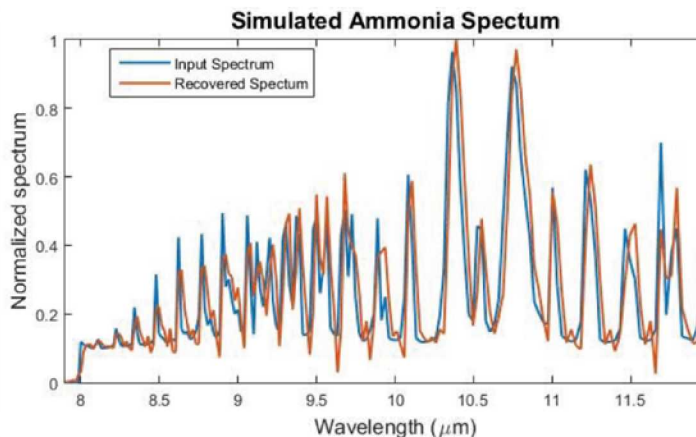
Polarization Grating  
Polarimeter



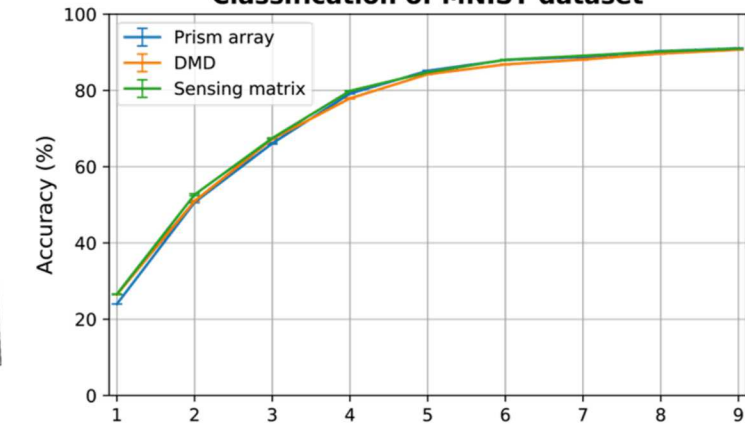
Simulated ammonium interferogram



Normalized spectrum



Classification of MNIST dataset





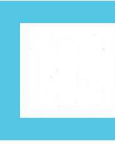
- **Publications**
  - Brian J. Redman, et al., "Measuring resolution degradation of long-wavelength infrared imagery in fog," *Opt. Eng.* **58**(5) 051806, 2019
- **Submitted**
  - Brian J. Redman, et al., "Simulating and characterizing an optimized snapshot channeled imaging polarimeter," *Opt. Express*, 2019
  - B. J. Redman, et al., "Performance evaluation of two optical architectures for task-specific compressive classification," *Optical Engineering*, 2019.
- **Conferences**
  - B. J. Redman, et al., "Active and passive long-wave infrared resolution degradation in realistic fog conditions," in *Situation Awareness in Degraded Environments*, **11019**, SPIE, 2019.
  - B. J. Redman, et al., "Design and evaluation of task-specific compressive optical systems," in *Defense and Commercial Sensing*, **10990**, SPIE, 2019.
  - B. J. Redman, et al. "Task-specific computational refractive element via two-photon additive manufacturing," in *Optical Design and Fabrication 2019 (Freeform, OFT)*, Optical Design and Fabrication 2019 (Freeform, OFT) , p. OT3A.5, Optical Society of America, 2019.
  - B. Redman, et al., "Optimizing a Compressive Imagers for Machine Learning Tasks," in *Asilomar Learning and Estimation in Imaging*, **11136**.
  - B. J. Redman, et al., "Hyperspectral vegetation identification at a legacy underground nuclear explosion test site," in *Chemical, Biological, Radiological, Nuclear, and Explosives (CBRNE) Sensing XX*, **11010**, SPIE, 2019.
- **Contributing**
  - G. C. Birch, B. J. Redman, A. L. Dagel, B. Kaehr, D. Dagel, C. F. LaCasse, T.-T. Quach, and M. Galiardi, "Characterization of 3D printed computational imaging element for use in task-specific compressive classification," in *Optics and Photonics for Information Processing XIII*, **11136**, pp. 63 – 73, SPIE, 2019.
  - M. P. Thornton, K. M. Judd, A. A. Richards, and B. J. Redman, "Multispectral short-range imaging through artificial fog," in *Infrared Imaging Systems: Design, Analysis, Modeling, and Testing XXX*, **11001**, pp. 340 – 350, SPIE, 2019.
  - J. D. van der Laan, B. J. Redman, J. W. Segal, K. Westlake, and J. B. Wright, "Testing active polarimetric imagers in fog (Conference Presentation)," in *Situation Awareness in Degraded Environments*, **11019**, SPIE, 2019.

The End

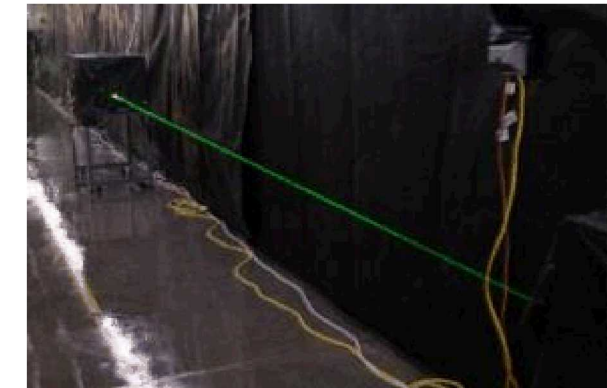
# Auxiliary slides



# Measuring fog droplet distribution



- Malvern Spratec
  - Volume distribution,  $v(d)$  in %
  - Narrow separation
  - Inhalation cell
- Transmissometer
  - Transmission,  $T$
  - Transmissometer separation,  $L_{trans}$
  - Long distance
- Mie scattering theory
  - Wavelength dependent
  - Particle size dependent
  - Extinction coefficient due to scattering,  $Q(d)$
- Products
  - Liquid water content, LWC
  - Number of droplets with given diameter,  $N(d)$
  - Meteorological optical range, MOR

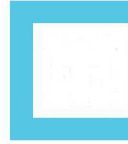


$$LWC = \frac{-2 \ln(T)}{3L_{trans} \sum_i \frac{Q(d_i) v(d_i)}{d_i}} \rho_{water}$$

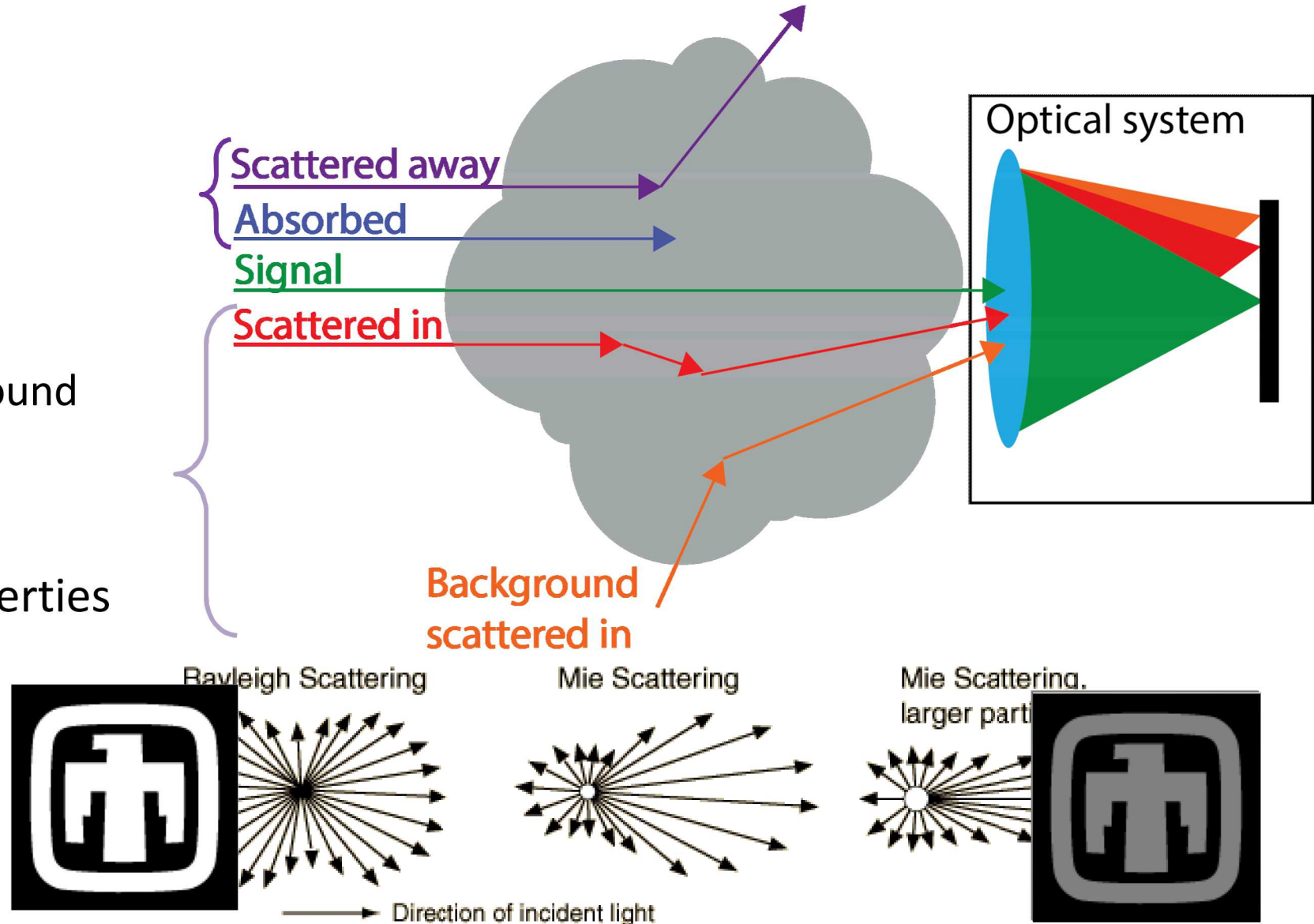
$$N(d) = \frac{LWC v(d)}{\frac{4\pi}{3} \left(\frac{d}{2}\right)^3}$$

$$MOR = L_{trans} \frac{\ln(0.05)}{\ln(T)}$$

# Multiple ways scattering degrades image quality



- **Attenuation**
  - Scattering
  - Absorption
- **Stray light**
  - Scattered from background
    - Signal independent
  - Scattered from scene
    - Causes **blurring**
- **Dependent on fog properties**
  - Particle size
  - Concentration
  - Wavelength
  - Geometry



Fog affects more than <sup>40</sup> transmission

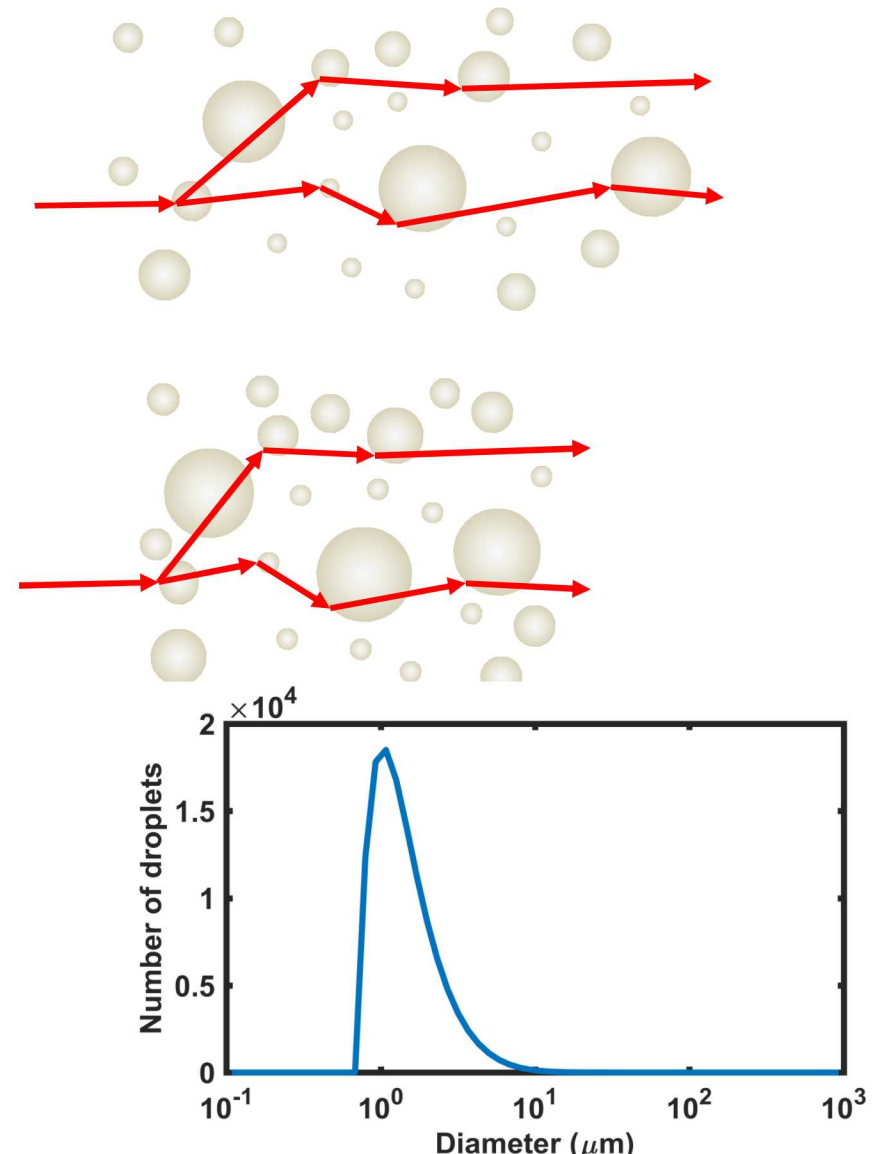
# Thick fog for long distance equivalent

- Scattering probability
  - Probability of hitting a droplet
- Beer-Lambert Law
  - Optical Thickness
  - Short distance through thick fog
  - longer distance through thinner fog
- Very dense particle concentration

## Equivalent distances through MOR=100m (ICAO) CATIIIc fog

Example case	Fog facility MOR (m)	Target distance (m)	Equivalent Distance to ICAO CATIIIc
<b>Passive Imaging Discussed in this Presentation</b>			
Thick fog	3	9 m	300 m
Moderate fog	6	9 m	150 m
Thin fog	15	9 m	60 m
<b>Full Length of Facility</b>			
Thick fog	3	55 m	1833 m
Moderate fog	6	55 m	917 m
Thin fog	15	55 m	367 m

Capable of very long equivalent distances



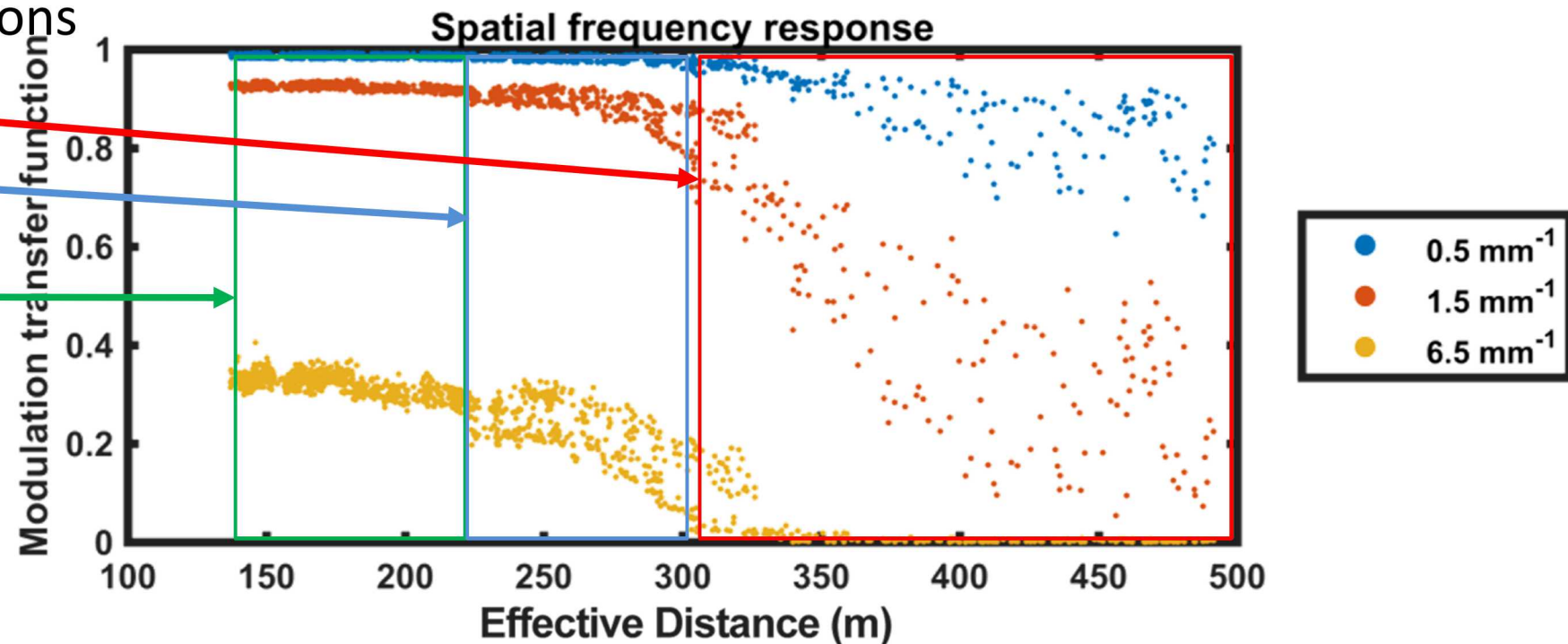
Brian J. Redman, et al., "Measuring resolution degradation of long-wavelength infrared imagery in fog," Opt. Eng. 58(5) 051806 (2019)

# Frequency response dependent on fog thickness

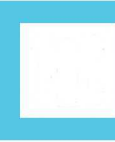


- Example frequencies of the MTF vs. fog thickness
- Effective distance through 92 m MOR
- Frequency response in regions

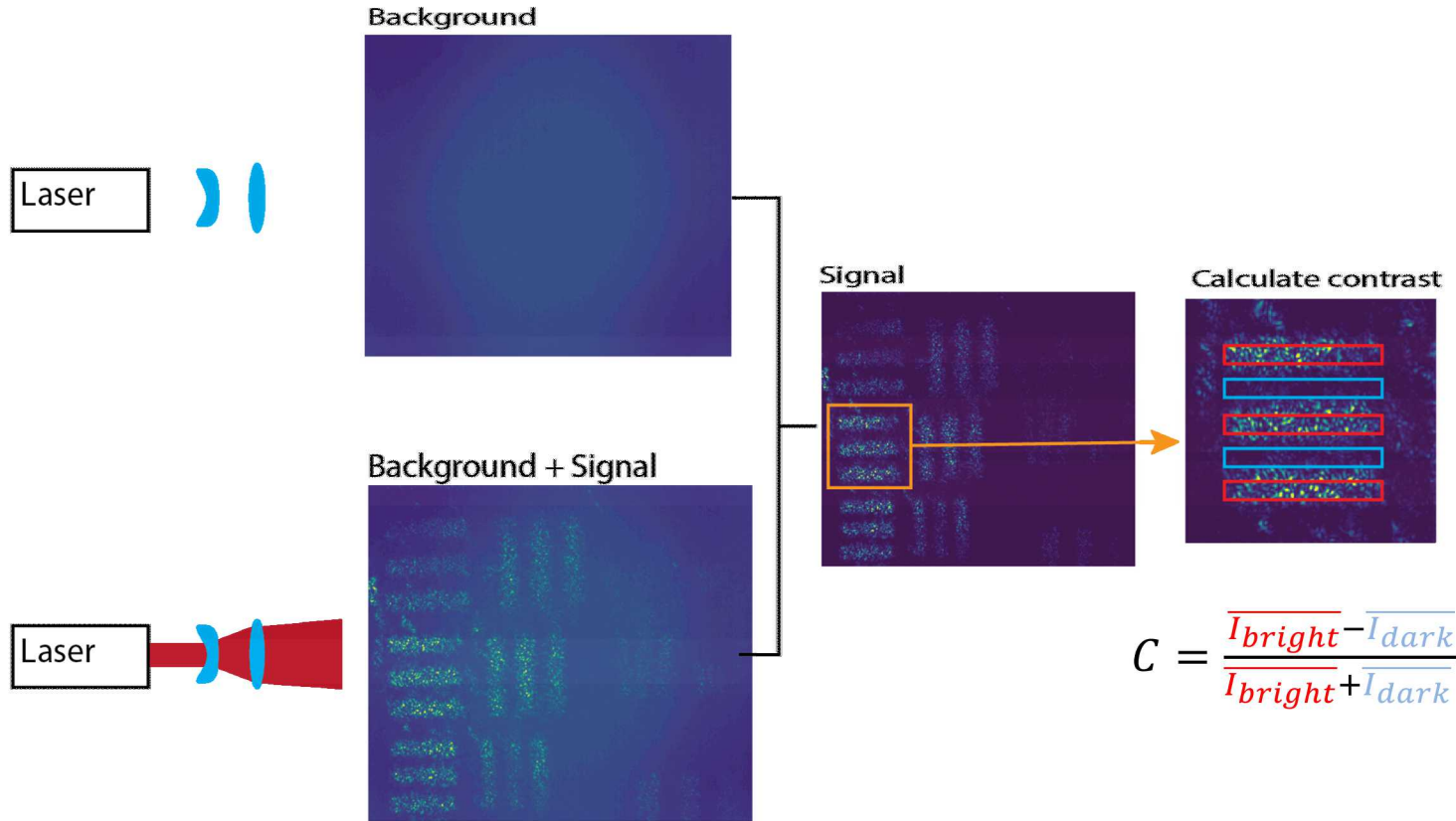
- Noise floor
- Frequency recovery
  - Slope frequency dependent
- Steady state



# Contrast measurement using active illumination

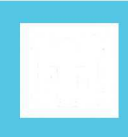


- Laser illumination
  - Speckle
  - Fourier analysis less effective
- Contrast transfer function
  - Averaging to reduce noise
- Shuttering
  - remove background

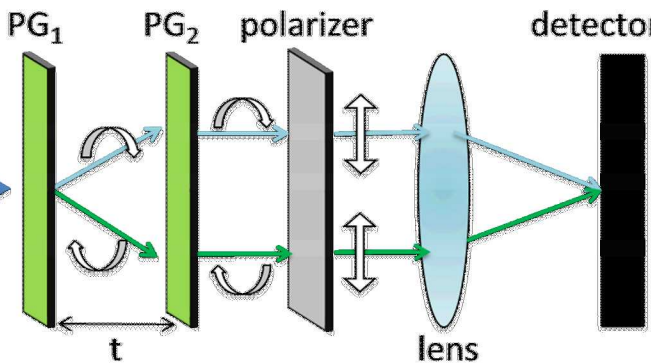


Contrast of speckle image requires averaging

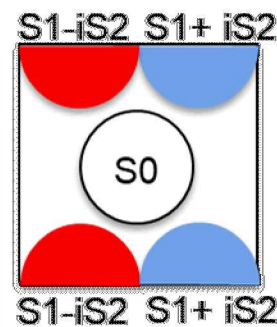
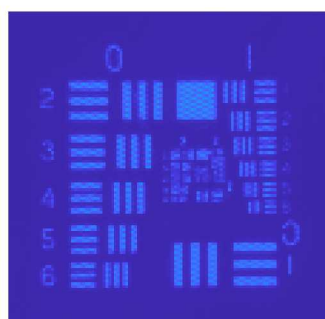
# Snapshot polarimeter



## Polarimeter

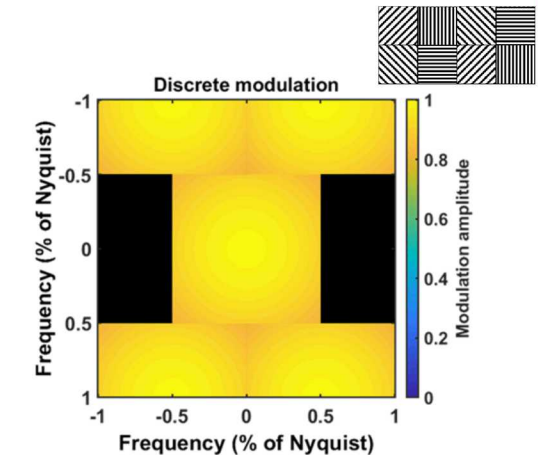
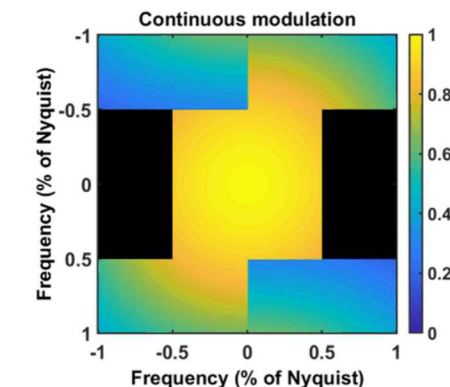


## Example image Fourier plane

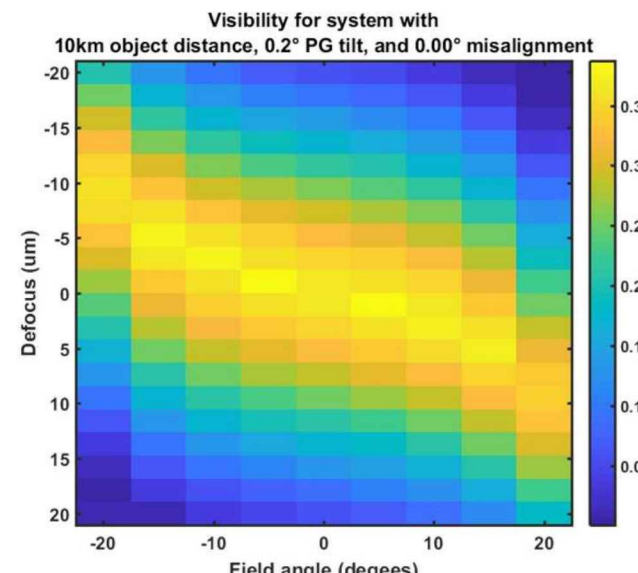
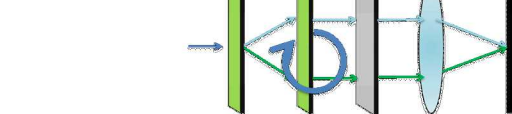
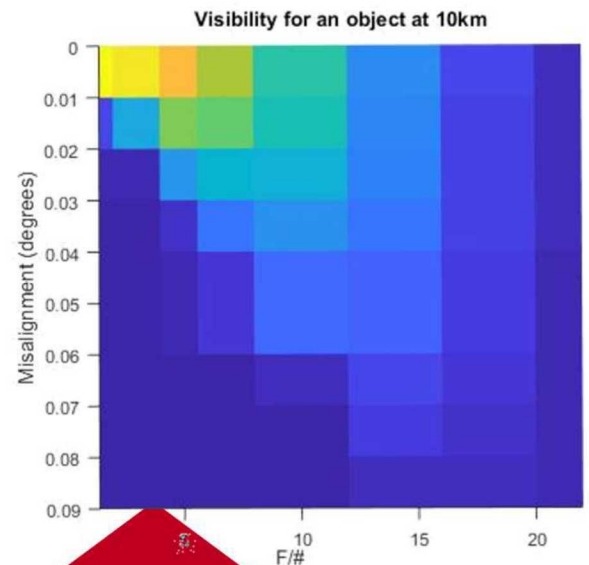
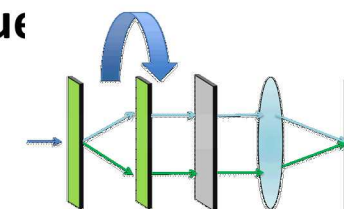


## Simulations

### Visibility reduction due to pixel sampling

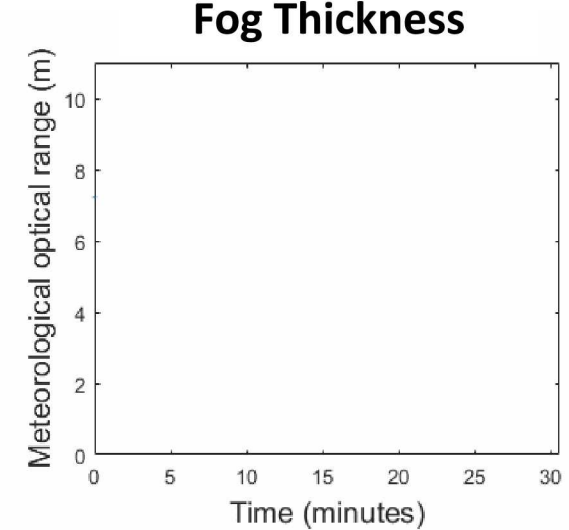
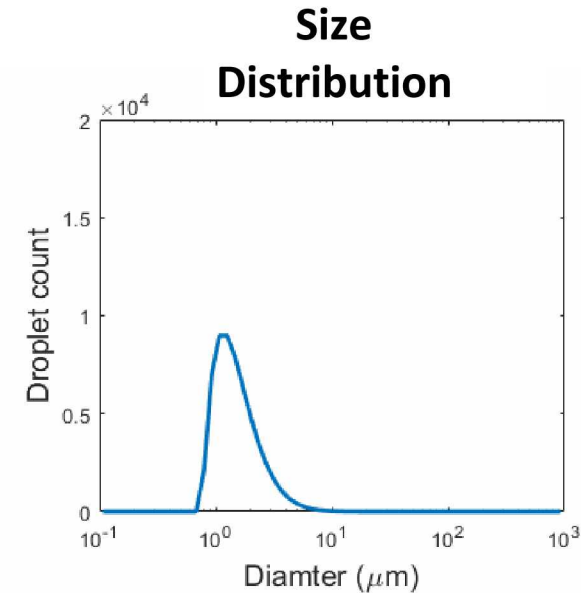
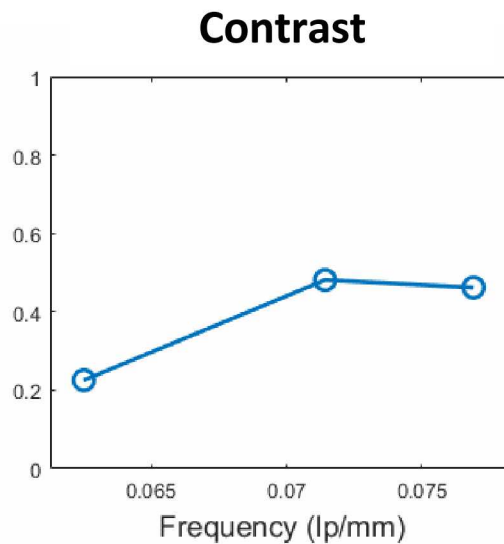
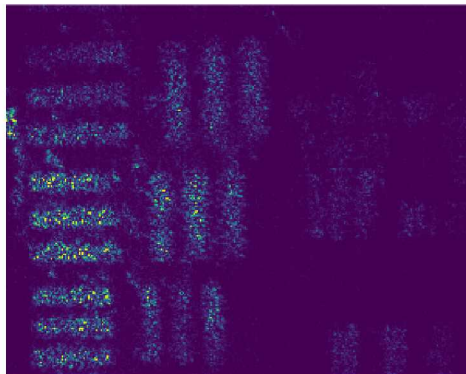


### Visibility reduction due to misalignment



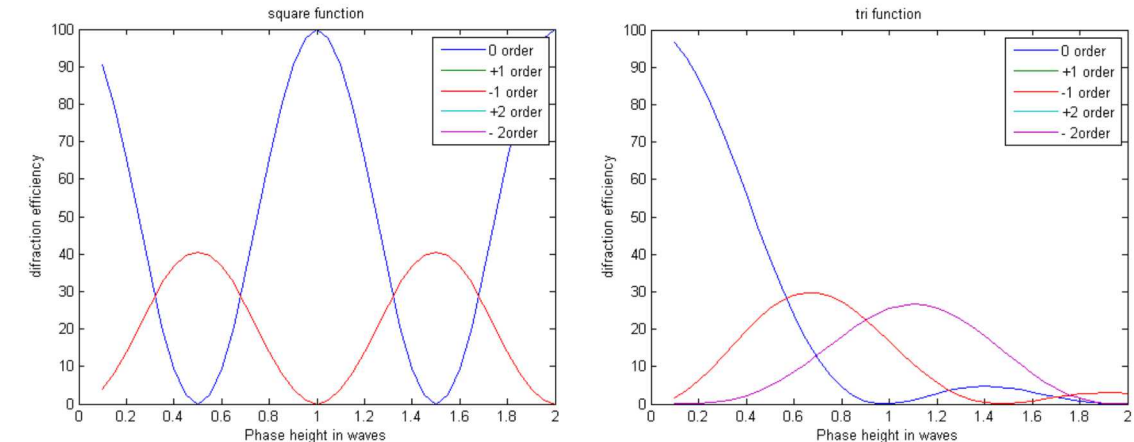
# Example active collect

- Target distance 3.0 m
- 1 generation cycle

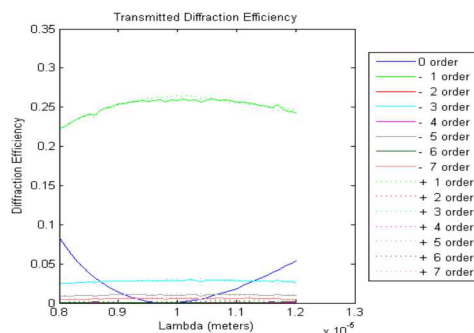


# Diffractive optic investigation

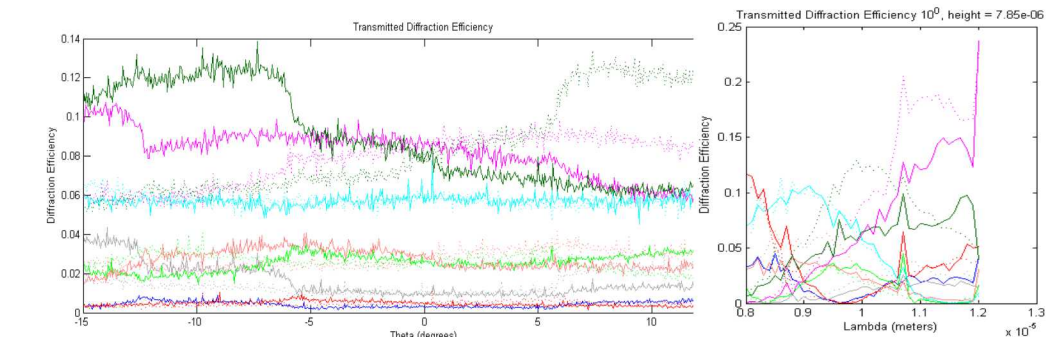
- Simulated the grating performance for
  - thin and thick
- Binary grating, and triangle profile
- RCWA for thick analysis



RCWA Binary



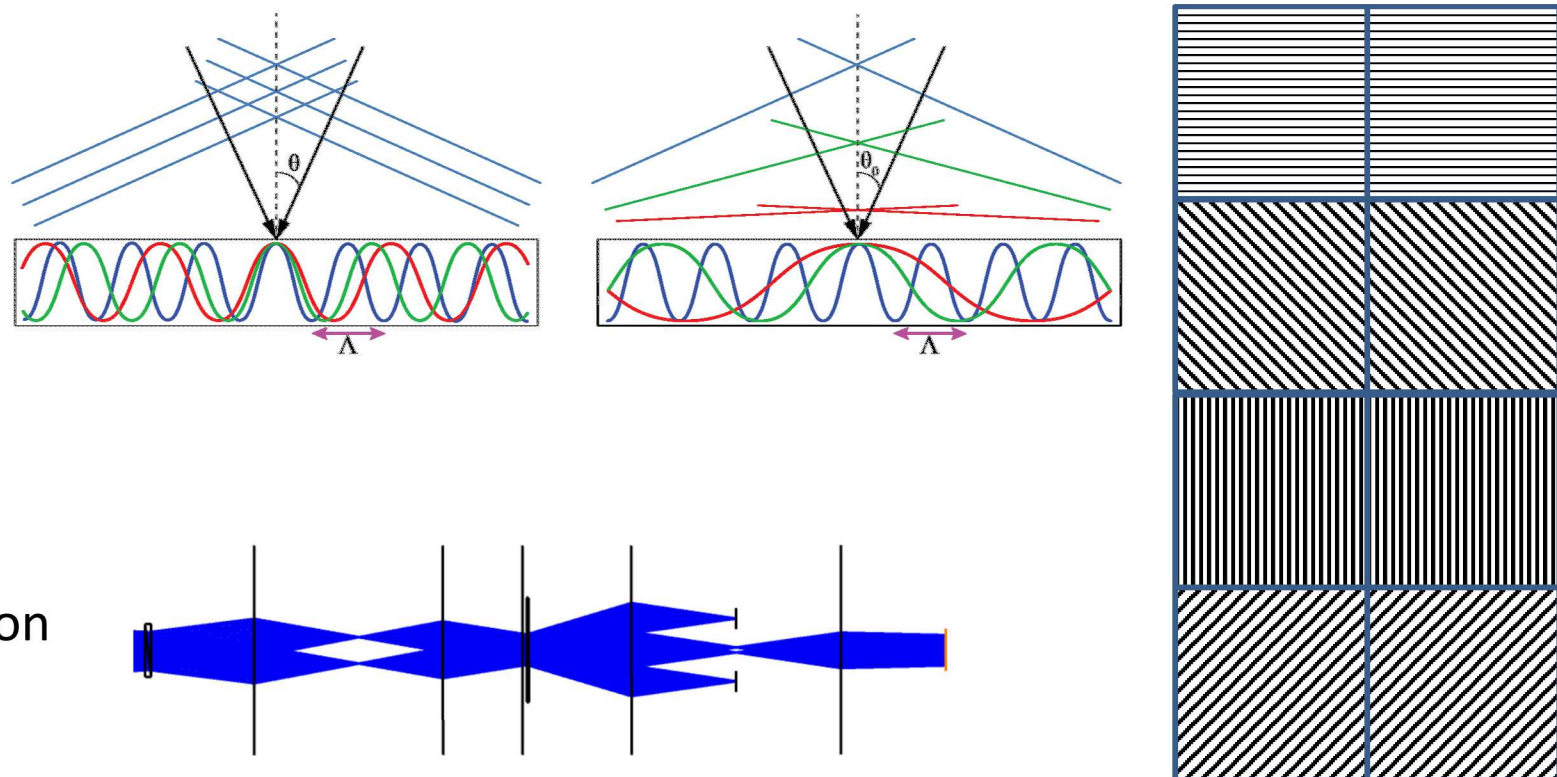
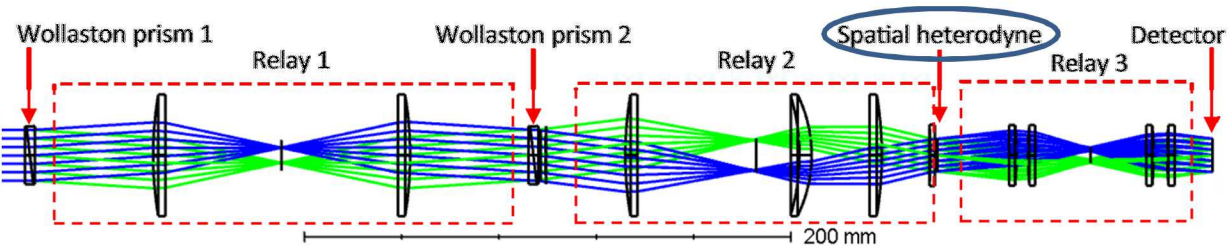
RCWA Tri



# Many separate elements as proof of concept for solid state Nomarski design



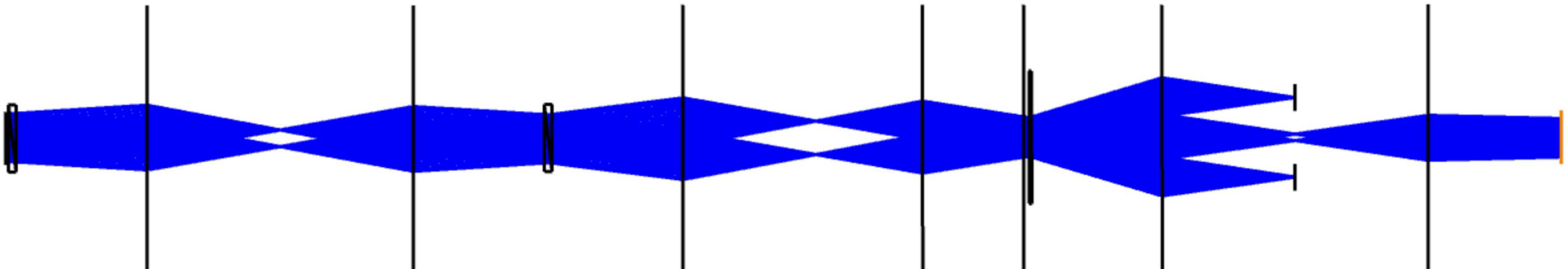
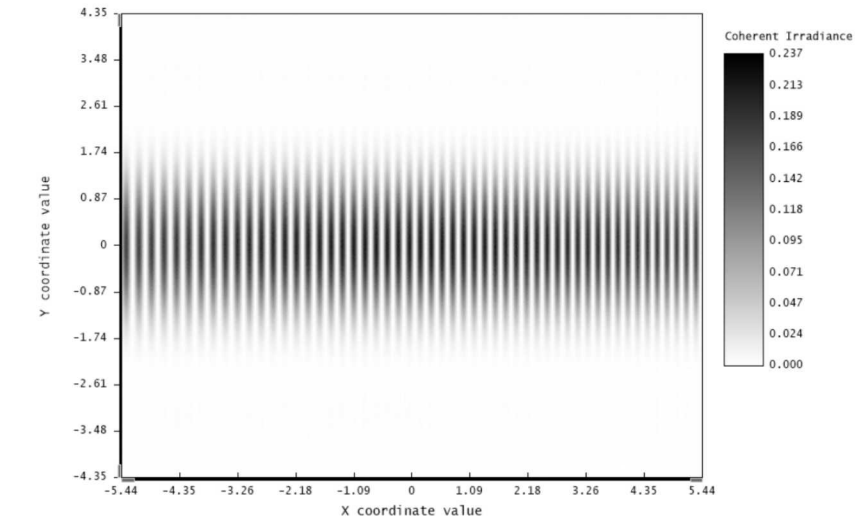
- Spatial heterodyning
  - Reduce spatial frequency
- Diffractive optic
  - Change angle of plane waves
  - Fourier filter to remove unwanted orders
- Patterned polarizer
  - Linear change of polarization angle
  - Multiply irradiance by sinusoid
  - Similar to AM radio demodulation



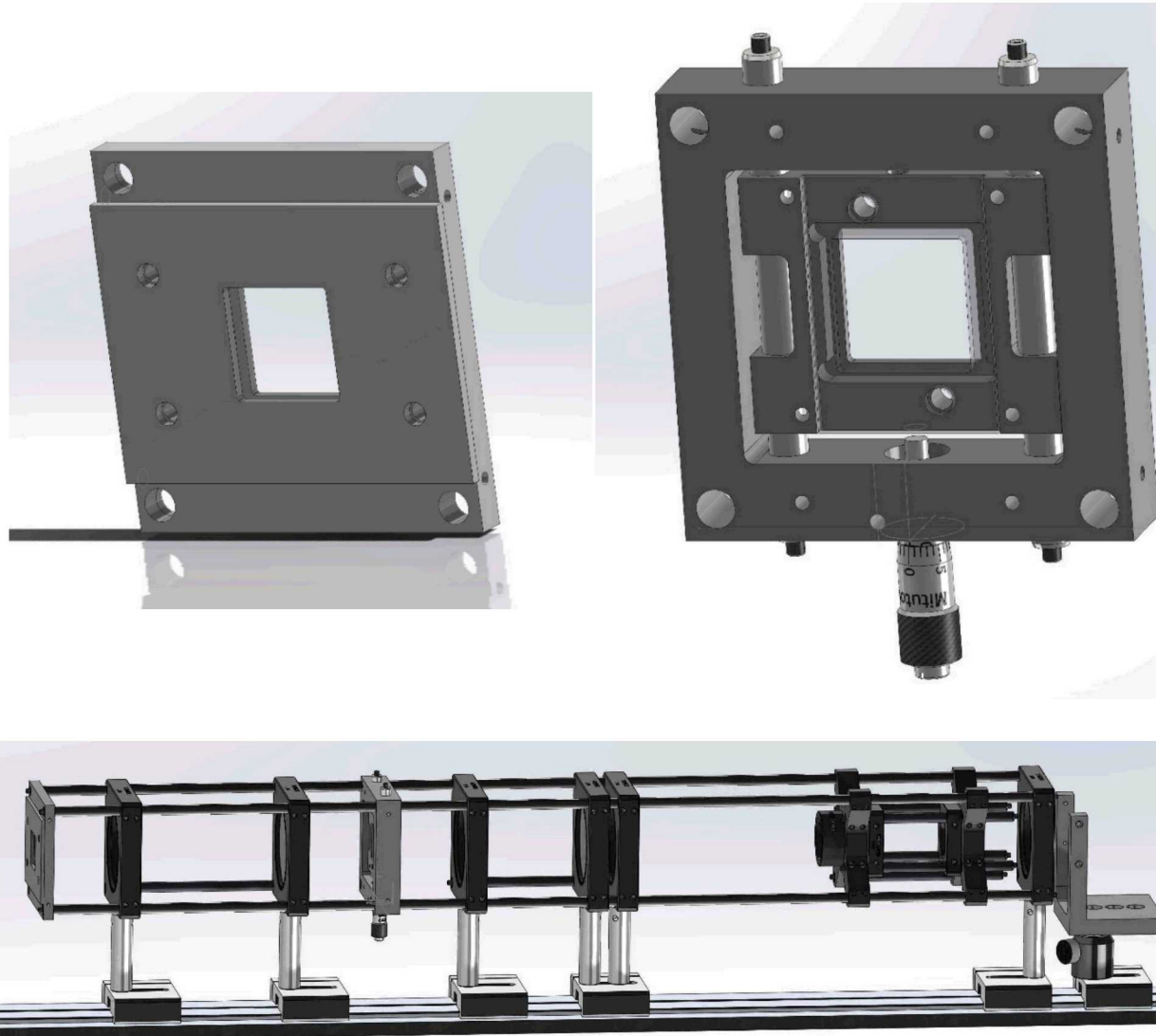
# Nonsequential Simulation



- Nonsequential OpticStudio ideally could simulate interferogram from multiple input angles without the need for Matlab
- Ideal on axis configuration gave an interferogram which seemed to have errors.



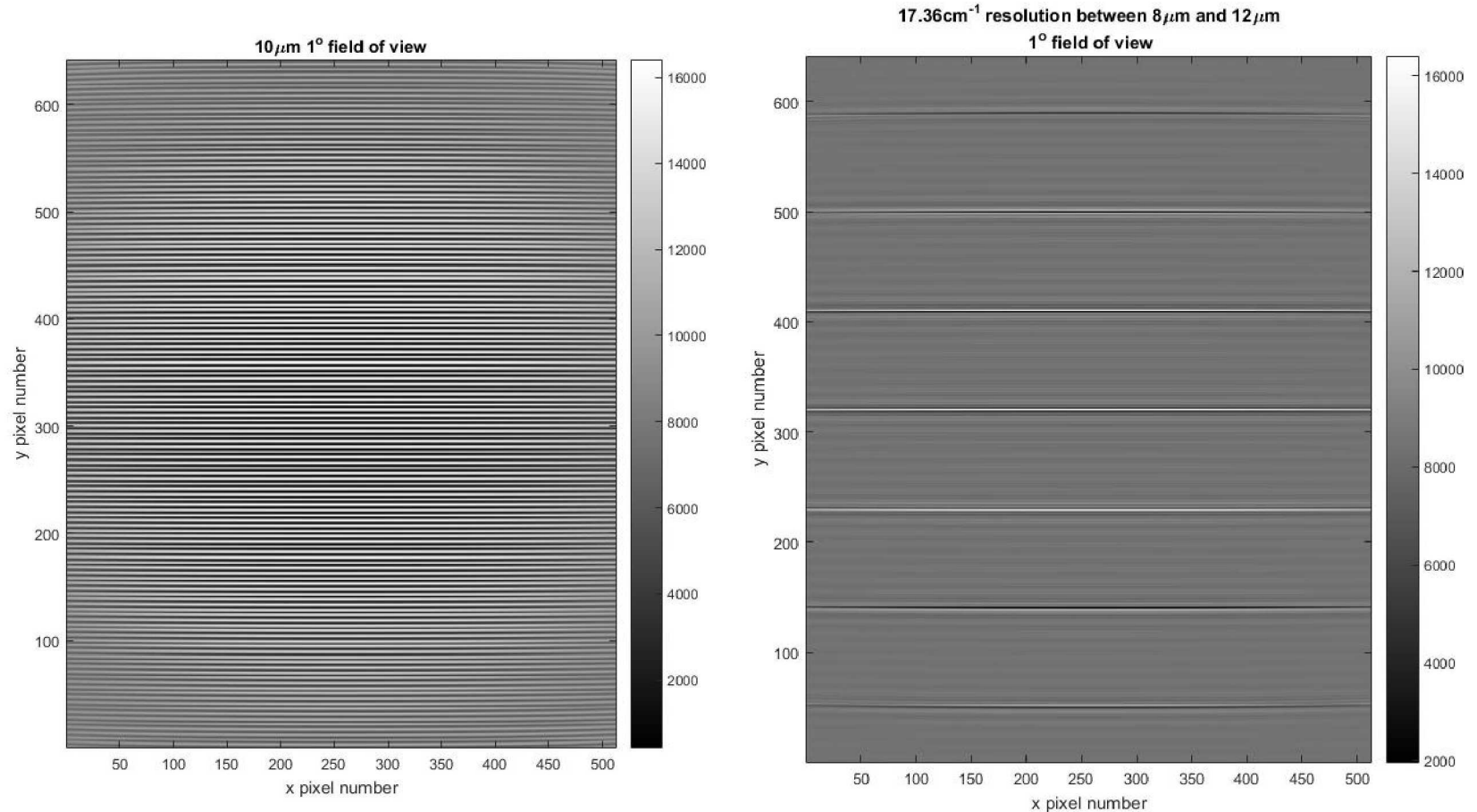
# Physical design



# Simulation of Interferogram



- A single wavelengths shows the slight blurring at the edges due to spatial incoherence
- Increasing the number of wavelengths dropped the visibility faster



# Weighting implemented using a DMD



- Digital micromirror device (DMD)

- Allows for dynamically setting sensing matrix **without changing hardware**

- At image plane

- Separating information

- DMD - channels separated, fields separated

- Detectors - channels separated, fields overlapping

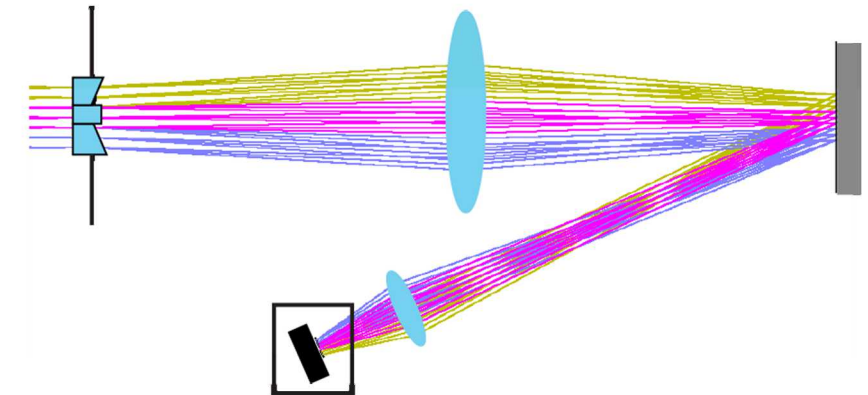
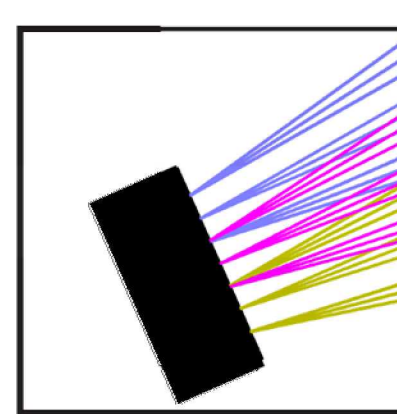
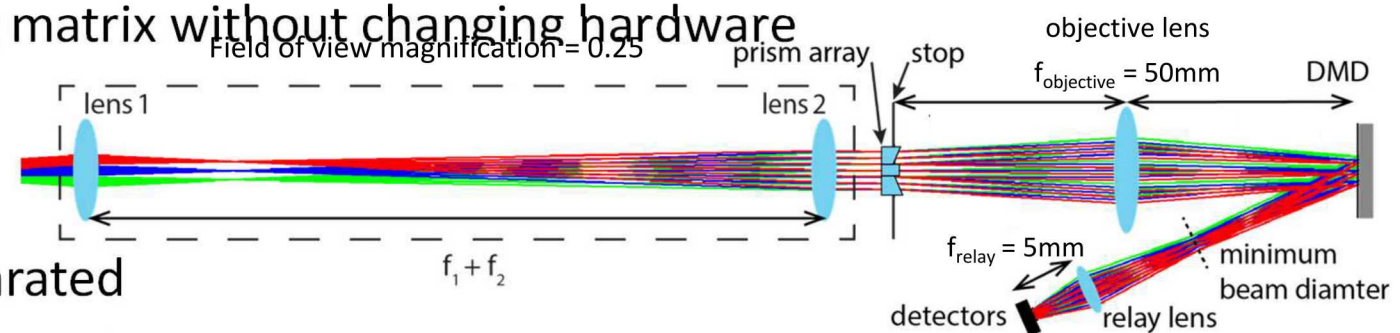
- Optimizing throughput

- Maximize magnification of detector

- Maximize field of view

- Constrained by DMD size

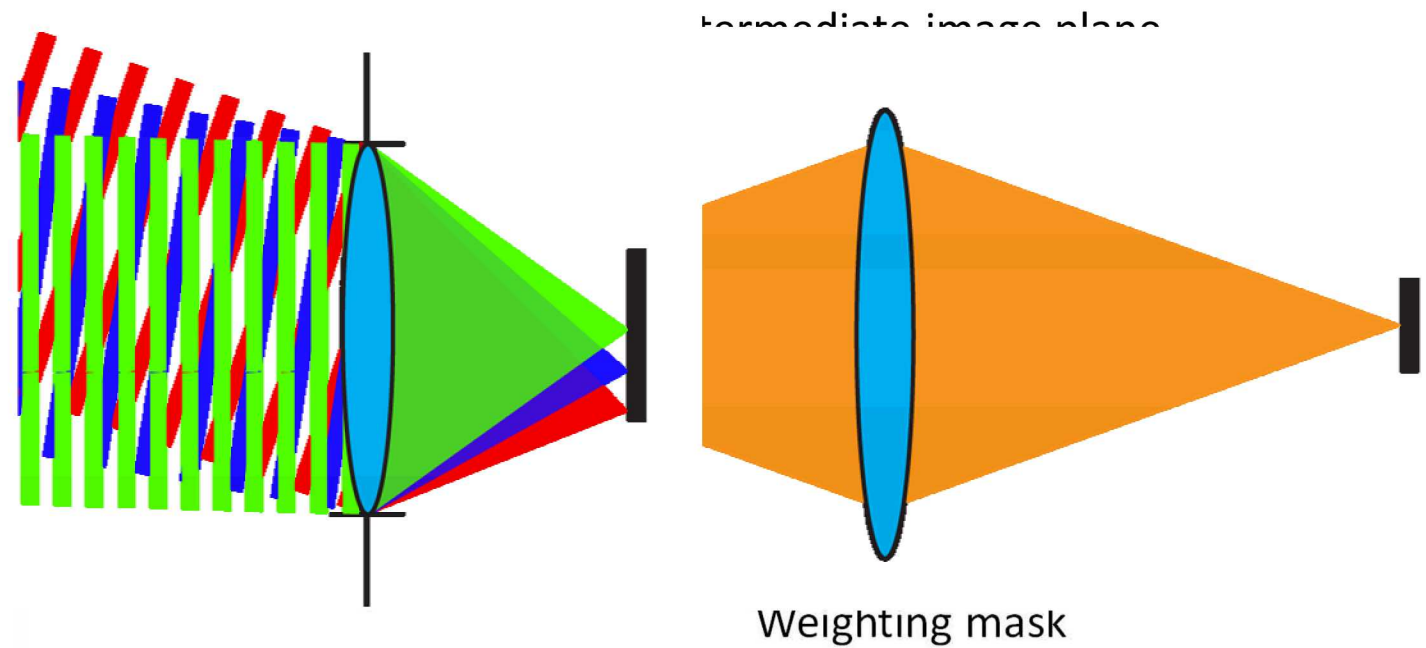
- Constrained by realistic lenses



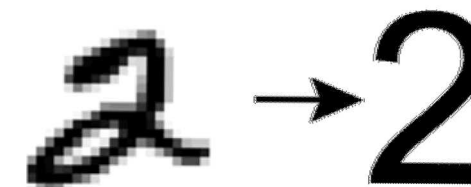
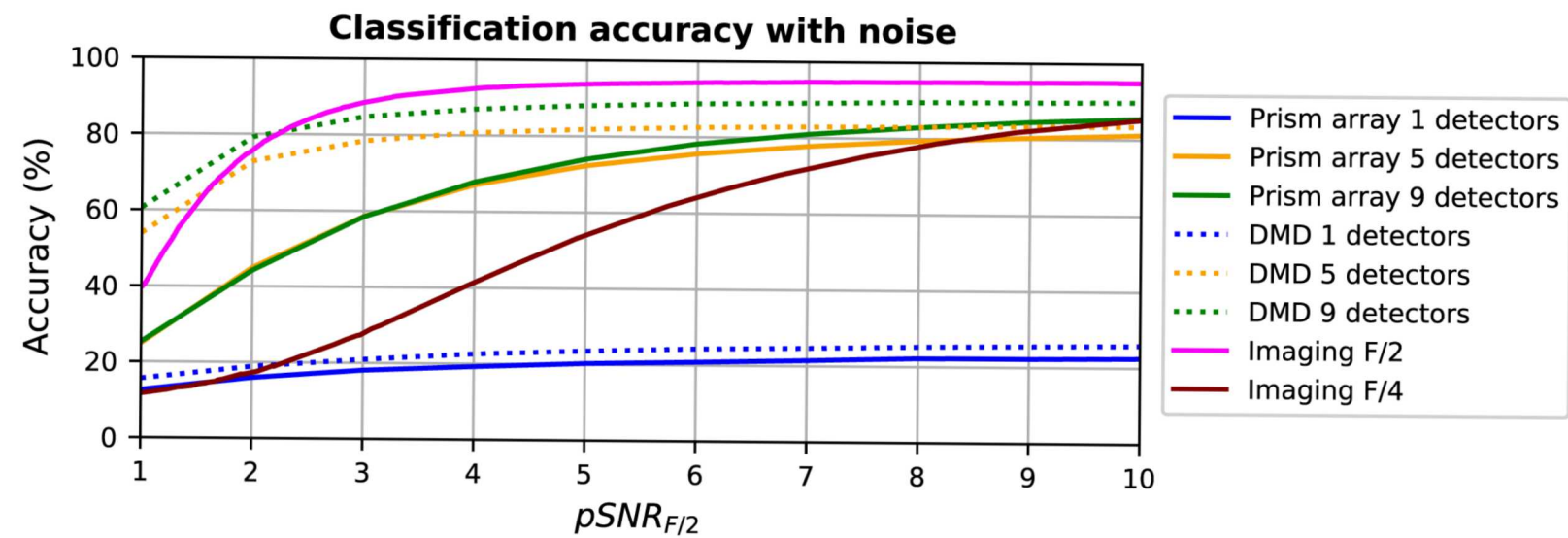
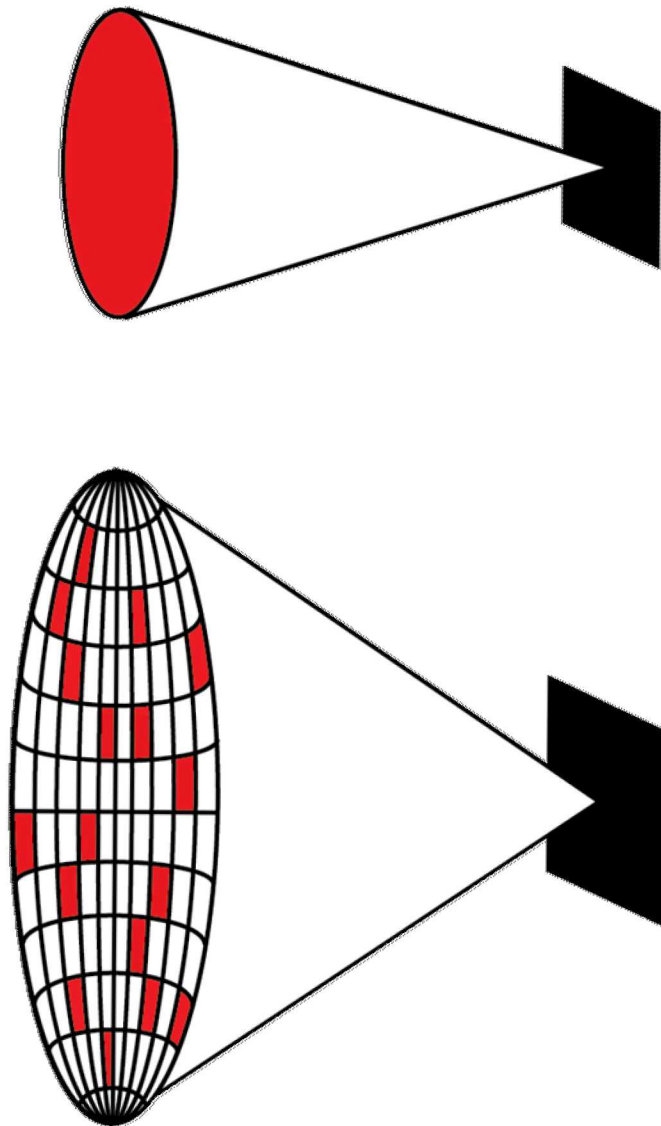
# Parallel measurements conventional optics



- Direct imaging
  - 1:1 mapping
- Image stop
  - Uniform irradiance at detector
- Telecentric
  - Intermediate image plane
  - Magnification independent of lens separation
- Division of aperture
  - Fields separated at intermediate image plane
  - Parallel measurements



# Radiometric modeling to compare performance between architectures

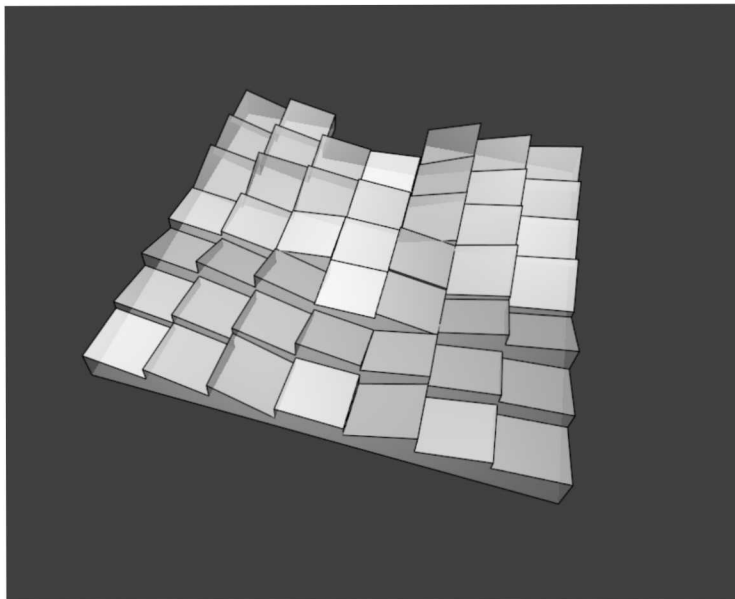


# Additive manufacturing of nontraditional component



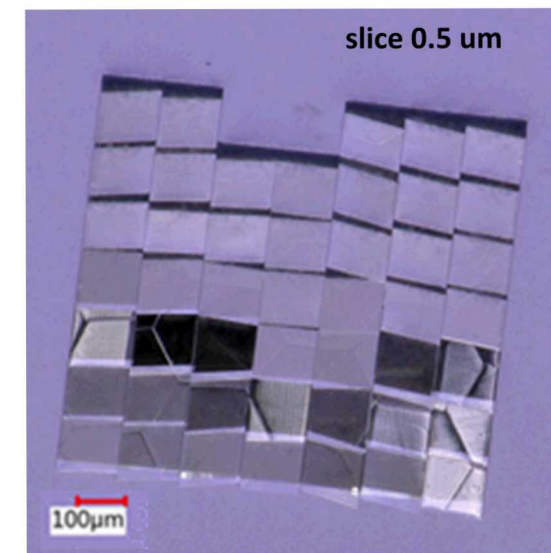
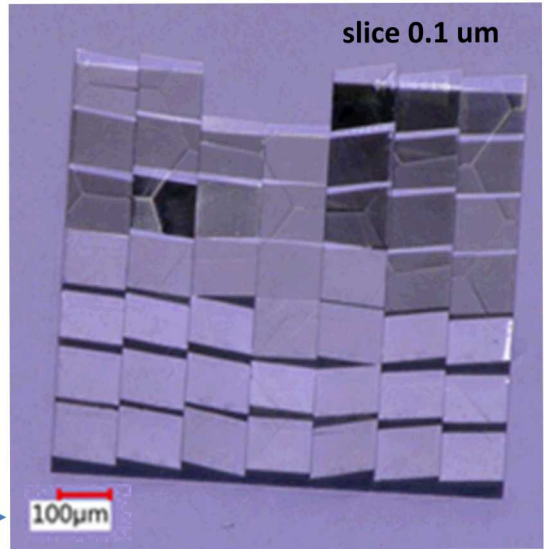
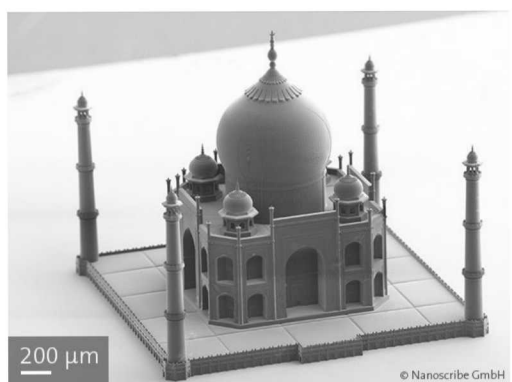
## Design of refractive optic

- Sharp edges
- Not feasible using traditional manufacturing



## Nanoscribe

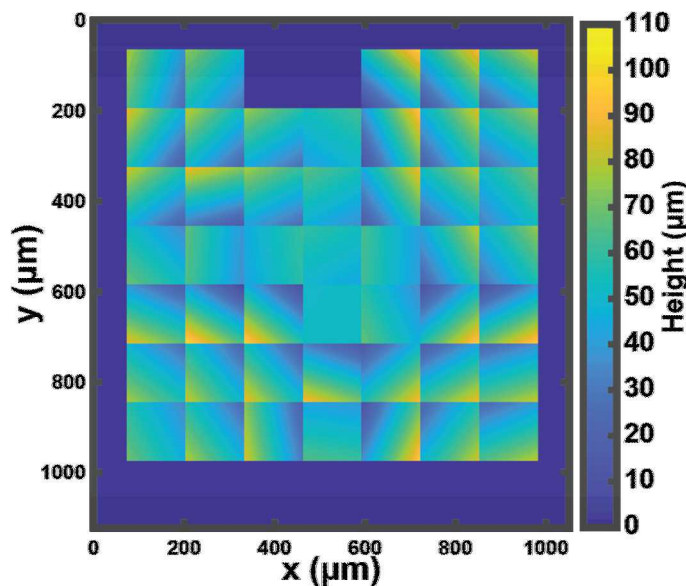
- 3D printer
- Two photon polymerization



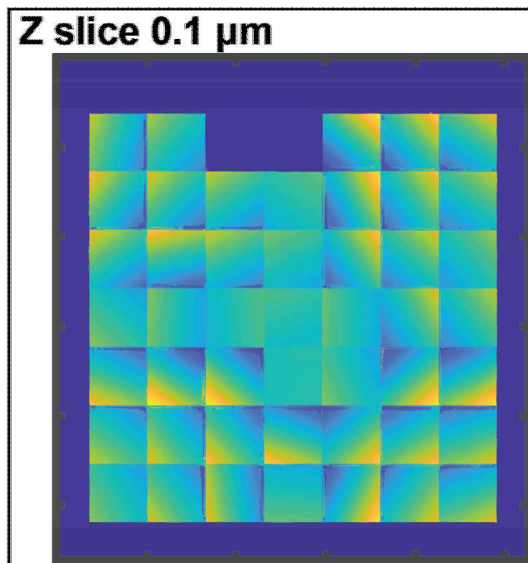
# Surface characterization – Binary Arrays



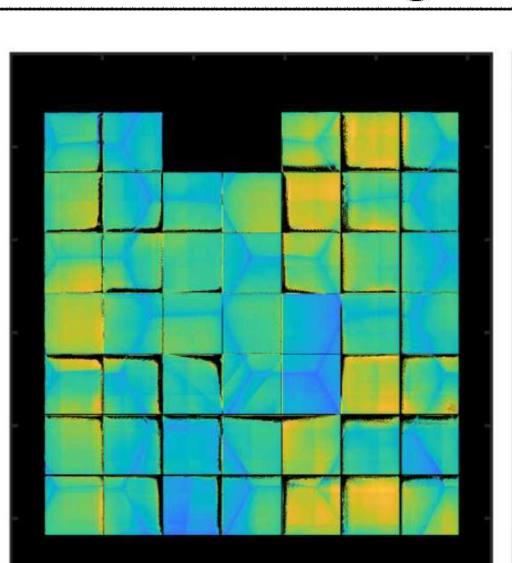
Design



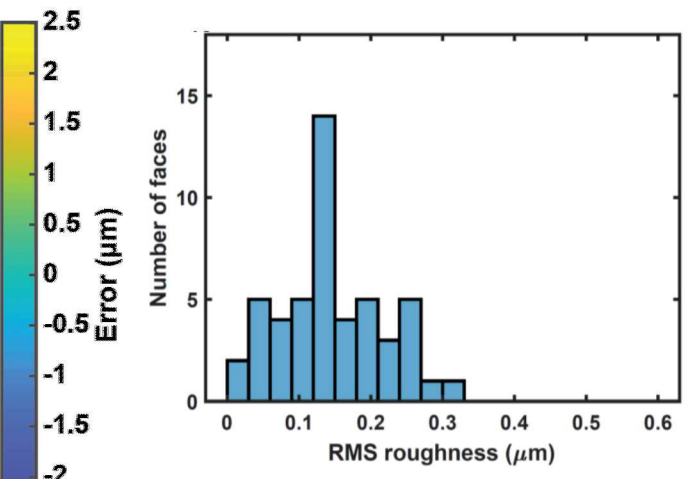
Measurement



Deviation from design

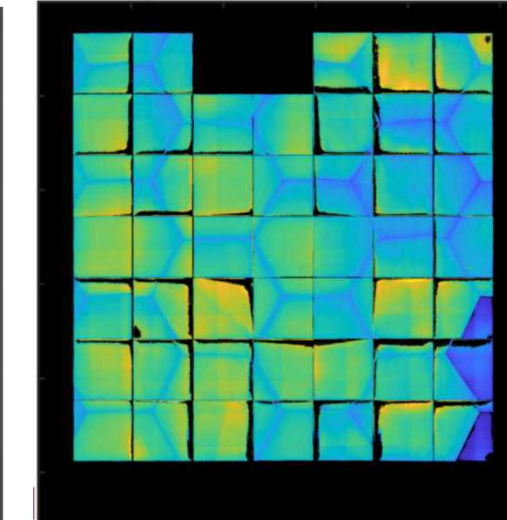
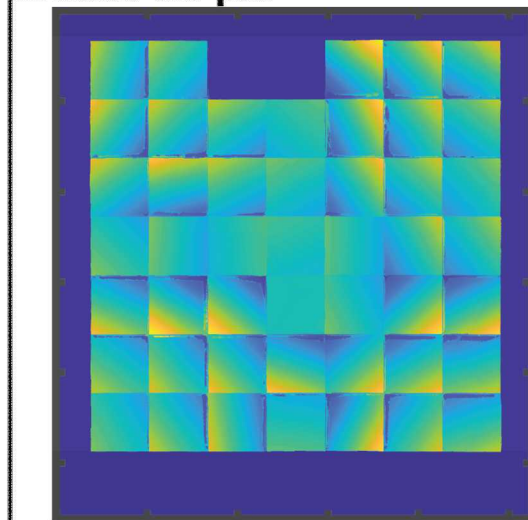


Surface roughness

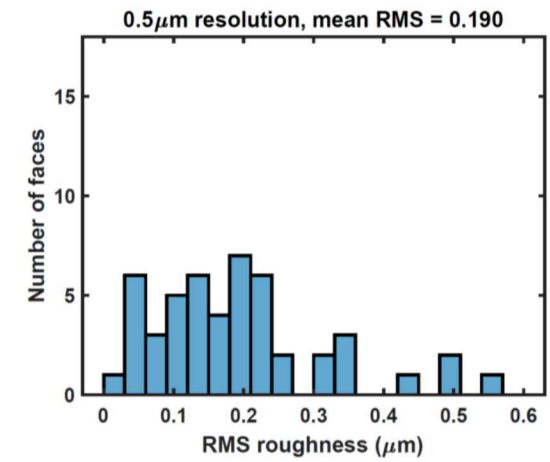


Mean RMS Roughness = 149 nm

**Z slice 0.5  $\mu\text{m}$**



0.5  $\mu\text{m}$  resolution, mean RMS = 0.190

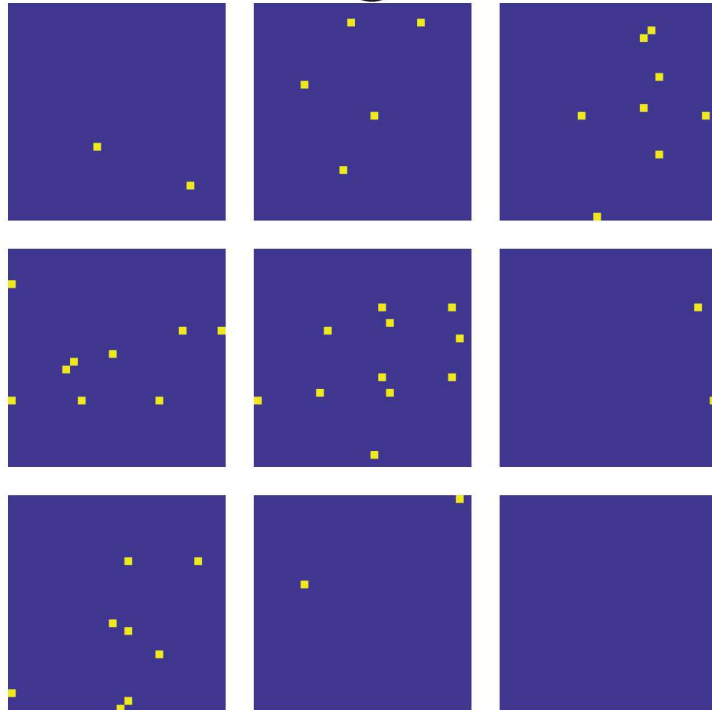


Mean RMS Roughness = 190 nm

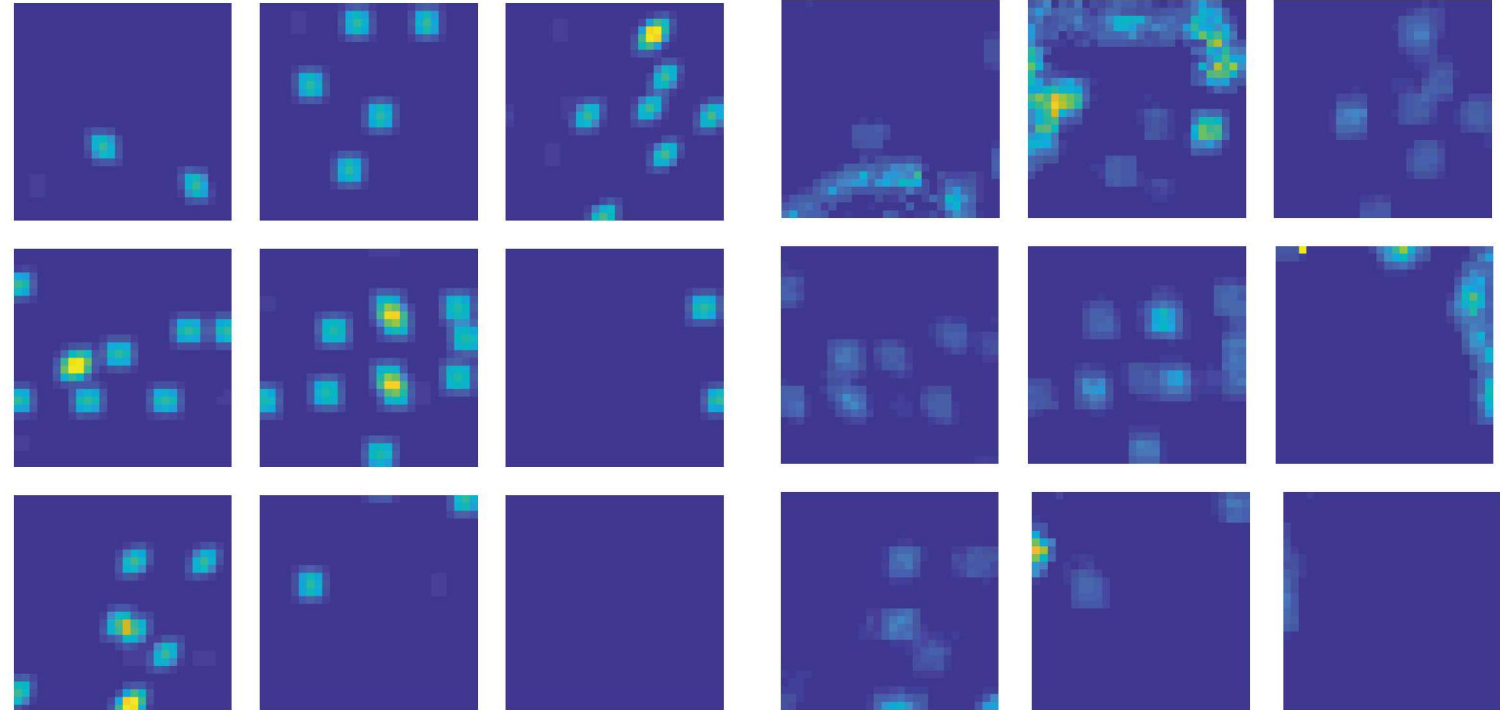
# Future Work – Complete system characterization



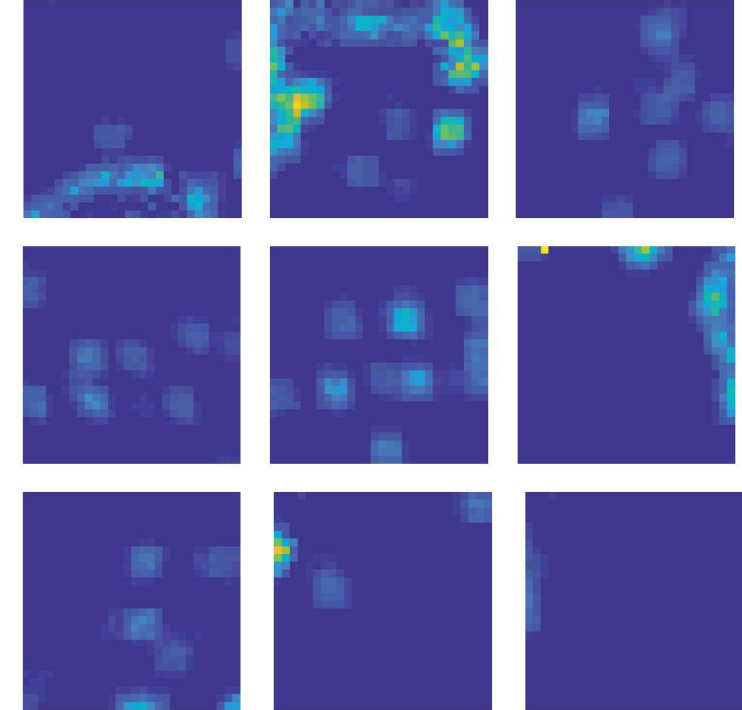
Sensing Matrix



Simulation



Measured



## Example printed prism

- Skirt to decrease masking requirements
- Multiple prisms to implement weighting
- Alignment pillars

